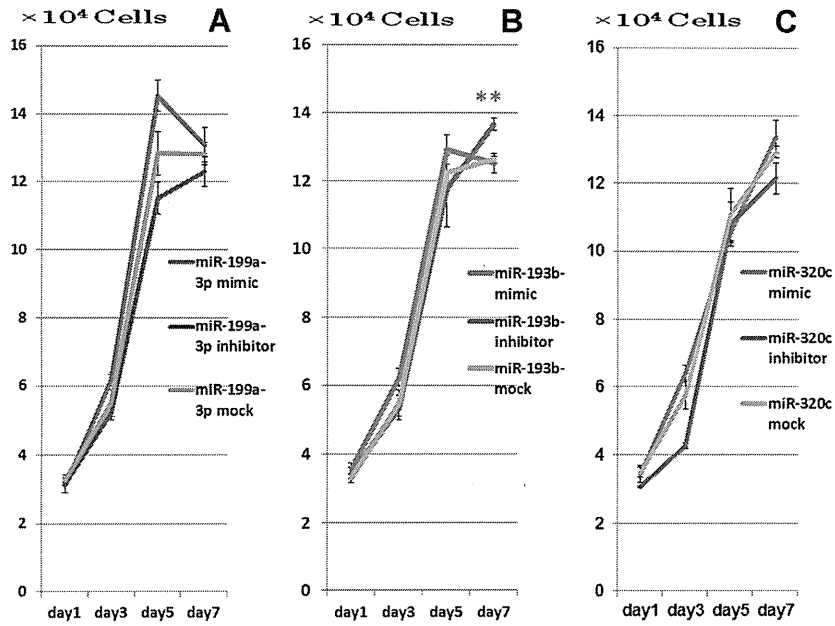

Figure 3. MTT assay. The cell proliferation potential did not differ between the mimic and the inhibitor group for miR-199a-3p (A) and miR-320c (C), but cell proliferation was upregulated significantly in the inhibitor group on day 7 (B). $^{**}p < 0.01$.

Table 5. MiRNA Expressions

	Fold Change		
	miR199a-3p Expession	miR193b Expression	miR320c Expression
Mimic	37.1533	141.9286	114.9257
Inhibitor	0.728932	0.372904	0.5014

Expression levels of the three miRNAs (miR-199a-3p, miR-193b, and miR-320c) isolated by the microarray analysis were increased by miScript miRNA Mimic, which had a similar function to the intrinsic mature miRNA. Expression levels were decreased by the miScript miRNA inhibitor, which specifically inhibited the function of the miRNA.

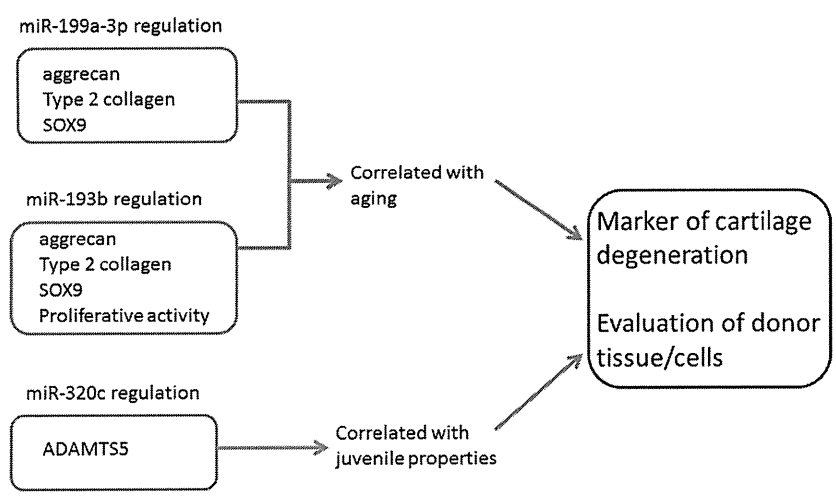

Figure 4. Three miRNAs (miR-199a-3p, miR-193b, and miR-320c) correlate with chondrocytes. MiR-199a-3p and miR-193b may be involved in chondrocyte aging by regulating aggrecan, Type 2 collagen, and SOX9, and miRNA-320c may be involved in the juvenile properties of chondrocytes by regulating ADAMTS5. MiR-199a-3p, miR-193b, and miR-320c may be useful for a marker of cartilage degeneration and evaluation as donor tissue of cartilage graft.

In summary, three types of miRNA whose expression correlates with age were identified in chondrocytes. These findings suggest that miR-199a-3p and miR-193b are involved in chondrocyte aging by regulating aggrecan and type 2 collagen, and that SOX9 and miRNA-320c are involved in the juvenile properties of chondrocytes by regulating ADAMTS5.

REFERENCES

1. Lewis BP, Burge CB, Bartel DP. 2005. Conserved seed pairing, often flanked by adenosines, indicates that thousands of human genes are microRNA targets. Cell 120:15–20.
2. Lin EA, Liu CJ. 2009. MicroRNAs in skeletogenesis. Front Biosci 14:2527–2764.
3. Kobayashi T, Lu J, Cobb BS, et al. 2008. Dicer-dependent pathways regulate chondrocyte proliferation and differentiation. Proc Natl Acad Sci USA 105:1949–1954.

4. Kongcharoensombat W, Nakasa T, Ishikawa M, et al. 2010. The effect of microRNA-21 on proliferation and matrix synthesis of chondrocytes embedded in atelocollagen gel. Knee Surg Sports Traumatol Arthrosc 18:1679–1684.
5. Miyaki S, Sato T, Inoue A. 2010. MicroRNA-140 plays dual roles in both cartilage development and homeostasis. Genes Dev 24:1173–1185.
6. Tardif G, Hum D, Pelletier JP, et al. 2009. Regulation of the IGFBP-5 and MMP-13 genes by the microRNAs miR-140 and miR-27a in human osteoarthritic chondrocytes. BMC Musculoskelet Disord 10:148.
7. Araldi E, Schipani E. 2010. MicroRNA-140 and the silencing of osteoarthritis. Genes Dev 24:1075–1080.
8. Yamasaki K, Nakasa T, Miyaki S, et al. 2009. Expression of microRNA-146a in osteoarthritis cartilage. Arthritis Rheum 60:1035–1041.
9. Iliopoulos D, Malizos KN, Oikonomou P, et al. 2008. Integrative microRNA and proteomic approaches identify novel osteoarthritis genes and their collaborative metabolic and inflammatory networks. PLoS ONE 3:e3740.
10. Miyaki S, Nakasa T, Otsuki S, et al. 2009. MicroRNA-140 is expressed in differentiated human articular chondrocytes and modulates interleukin-1 responses. Arthritis Rheum 60:2723–2730.
11. Chan SP, Slack FJ. 2006. microRNA-mediated silencing inside P-bodies. RNA Biol 3:97–100.
12. Chen CZ, Li L, Lodish HF, et al. 2006. MicroRNAs modulate hematopoietic lineage differentiation. Science 303:83–86.
13. Esau C, Kang X, Peralta E, et al. 2004. MicroRNA-143 regulates adipocyte differentiation. J Biol Chem 279:52361–52365.
14. Harris TA, Yamakuchi M, Ferlito M, et al. 2008. MicroRNA-126 regulates endothelial expression of vascular cell adhesion molecule 1. Proc Natl Acad Sci USA 105:1516–1521.
15. Krichevsky AM, Sonntag KC, Isacson O, et al. 2006. Specific microRNAs modulate embryonic stem cell-derived neurogenesis. Stem Cells 24:857–864.
16. Sempere LF, Freemantle S, Pitha-Rowe I, et al. 2004. Expression profiling of mammalian microRNAs uncovers a subset of brain-expressed microRNAs with possible roles in murine and human neuronal differentiation. Genome Biol 5:R13.
17. Yi R, O'Carroll D, Pasolli HA, et al. 2008. Morphogenesis in skin is governed by discrete sets of differentially expressed microRNAs. Nat Genet 38:356–362.
18. Zhao Y, Samal E, Srivastava D. 2002. Serum response factor regulates a muscle-specific microRNA that targets Hand2 during cardiogenesis. Nature 436:214–220.
19. Lee RC, Feinbaum RL, Ambros V, et al. 1993. The C. elegans heterochronic gene lin-4 encodes small RNAs with antisense complementarity to lin14. Cell 75:843–854.
20. Berezikov E, Guryev V, van de Belt J, et al. 2005. Phylogenetic shadowing and computational identification of human microRNA genes. Cell 120:21–24.
21. Lin EA, Kong L, Bai XH, et al. 2009. miR-199a, a bone morphogenic protein 2-responsive microRNA, regulates chondrogenesis via direct targeting to Smad1. J Biol Chem 284:11326–11335.
22. Lin L, Shen Q, Zhang C, et al. 2011. Assessment of the profiling microRNA expression of differentiated and dedifferentiated human adult articular chondrocyte. J Orthop Res 29: 1578–1584.
23. Ling HY, Ou HS, Feng SD, et al. 2009. Changes in microRNA (miR) profile and effects of miR-320 in insulin-resistant 3T3-L1 adipocytes. Clin Exp Pharmacol Physiol 36:e32–e39.
24. Kubo H, Shimizu M, Taya Y, et al. 2009. Identification of mesenchymal stem cell (MSC)-transcription factors by microarray and knockdown analyses, and signature molecule-marked MSC in bone marrow by immunohistochemistry. Genes Cells 14:407–424.
25. Yates KE. 2006. Identification of *cis* and *trans*-acting transcriptional regulators in chondroinduced fibroblasts from the pre-phenotypic gene expression profile. Gene 377:77–78.

Biomaterials 33 (2012) 5278–5286

Contents lists available at SciVerse ScienceDirect

Biomaterials

journal homepage: www.elsevier.com/locate/biomaterials

Repair of articular cartilage defect with layered chondrocyte sheets and cultured synovial cells

Satoshi Ito [a], Masato Sato [a,*], Masayuki Yamato [b], Genya Mitani [a], Toshiharu Kutsuna [a], Toshihiro Nagai [a], Taku Ukai [a], Miyuki Kobayashi [a], Mami Kokubo [a], Teruo Okano [b], Joji Mochida [a]

[a] Department of Orthopaedic Surgery, Surgical Science, Tokai University School of Medicine, 143 Shimokasuya, Isehara, Kanagawa 259-1193, Japan
[b] Institute of Advanced Biomedical Engineering and Science, Tokyo Women's Medical University, 8-1 Kawada-cho, Shinjuku-ku, Tokyo 162-8666, Japan

ARTICLE INFO

Article history:
Received 23 January 2012
Accepted 25 March 2012
Available online 30 April 2012

Keywords:
Chondrocyte
Animal model
Cell culture
Transplantation

ABSTRACT

In this study, we investigate the effects of treatment with layered chondrocyte sheets and synovial cell transplantation. An osteochondral defect was created of 48 Japanese white rabbits. In order to determine the effects of treatment, the following 6 groups were produced: (A) synovial cells (1.8×10^6 cells), (B) layered chondrocyte sheets (1.7×10^6 cells), (C) synovial cells (3.0×10^5 cells) + layered chondrocyte sheets, (D)synovial cells (6.0×10^5 cells) + layered chondrocyte sheets, (E)synovial cells (1.2×10^6 cells) + layered chondrocyte sheets, (F) osteochondral defect. Layered chondrocyte sheets and synovial cells were transplanted, sacrificed four and 12 weeks postoperatively. An incapacitance tester (Linton) was used to find trends in the weight distribution ratio of the damaged limbs after surgery. Sections were stained with Safranin-O. Repair sites were evaluated using ICRS grading system. In groups (A) to (E), the damaged limb weight distribution ratio had improved. The repair tissue stained positively with Safranin-O. Four and 12 weeks after surgery, groups (A) to (E) exhibited significantly higher scores than group (F), and groups (D) and (E) exhibited significantly higher scores than groups (A) and (B). This suggests the efficacy of combining layered chondrocyte sheets with synovial cells.

1. Introduction

Articular cartilage is avascular tissue nourished by synovial fluid. Articular cartilage shows limited capacity for regeneration after degeneration or injury [1],and leads to osteoarthritis ("OA"). As societies age, much attention is being focused on OA prevention and countermeasures. Treatments for osteochondral defects have included to date: micro fracturing [2–4], mosaicplasty [5–7] and endoprosthetic joint replacement. Beginning with the report by Brittberg et al [11] of autologous chondrocyte implantation (ACI), as a result of development in tissue engineering research a variety of cultured cell graft techniques [11–25] have become the subject of further enquiry. Microfracture surgery and drilling are techniques that encourage natural repair by filling osteochondral defects with marrow-derived repair cells. Normally, an osteochondral defect will induce the production of marrow-derived repair cells [8]. Osteochondral defects are generally thought to be ultimately replaced by subchondral bone after infiltration by blood vessels during endochondral ossification of chondrocytes from multipotent, marrow-derived MSC [9,10].Nagai et al. fabricated tissue-engineered cartilage without a scaffold and reported that chondrocyte plates were effective at repairing tissue in animal experiments [21,22]. The usefulness of temperature-responsive culture dishes was reported by Okano et al. [26,27]. Previously, myocardial, corneal and other types of cell sheets have been reported [28–30].

We are continuing to conduct animal experiments with the aim of developing clinical applications for articular cartilage treatment using cell sheets with adhesive properties that were obtained from temperature-responsive culture dishes. Kaneshiro et al. achieved good treatment outcomes by transplantation chondrocyte sheets into partial defect models [31]. Furthermore, Mitani et al. investigated chondrocyte sheets molecular-biologically and immunohistochemically, and examined the chondrocyte repair process [32].

Cartilage repair using synovial cell grafts has been carried out. Hunziker et al have reported synovial cells played an important role in the repair of the cartilage defects [43], and Koga et al have created osteochondral defects in rabbit knee joints and reported good results from grafts of synovium-derived mesenchymal stem cells used in conjunction with periosteum [44]. However, Ando et al investigated repair of articular cartilage using chondrocytes and

* Corresponding author. Tel.: +81 463 93 1121; fax: +81 463 96 4404.
E-mail address: sato-m@is.icc.u-tokai.ac.jp (M. Sato).

0142-9612/$ – see front matter © 2012 Elsevier Ltd. All rights reserved.
doi:10.1016/j.biomaterials.2012.03.073

found that the superficial layers of the repaired tissue included fibrous tissue [33]. Further investigation into osteochondral defects using larger animals has been carried out by Ebihara et al using the minipig model and they have previously reported the efficacy of repairs using layered chondrocyte sheets [36]. In order to solve the problem of fibrous tissue being included in the superficial layer in this experiment we investigated the combined use of synovial cells and layered chondrocyte sheet for the repair of articular cartilage.

2. Materials and methods

All procedures using animals in this study were performed in accordance with the Guide for the Care and Use of Laboratory Animals (NIH Publication No. 85-23, revised 1996) published by the National Institutes of Health, USA, and the Guidelines of Tokai University on Animal Use.

2.1. Temperature-responsive culture dishes

The temperature-responsive culture dishes are coated with Poly(N-isopropylacrylamide) which can change between hydrophilic and hydrophobic depending on the temperature, and was developed by Okano et al. [26,27]. It enables the recovery of sheets of cells without endangering the extracellular matrix, and damage to cells through the use of Trypsin can be avoided. The culture dishes were sterilized using ethylene oxide gas [34]. This product is currently being sold by CellSeed Inc.

2.2. Harvesting of chondrocytes and synovial cells from Japanese white rabbits

Four Japanese white rabbits aged 16–18 weeks old and weighing about 3 kg were used as the source of articular chondrocytes and synovial cells. The chondrocytes were harvested from the rabbits' femurs, and the synovial cells were harvested from inside their knee joints. After the cells were enzymatically isolated, the chondrocytes were seeded on temperature-responsive inserts and the synovial cells in temperature-responsive culture dishes, and the cells were cocultured. We understand the need for very long culture times, due to the small amount of chondrocytes capable of being harvested from cartilage and their poor proliferative properties. Huch et al have reported on the interaction between cell types based on a coculture of human synovial cells and chondrocytes [35]. This time, we seeded temperature-responsive inserts with chondrocytes using the method reported by Ebihara, and seeded temperature-responsive culture dishes with synovial cells and cocultured them via the inserts [36]. The results were that there was a significant increase in the activation of proliferation of cells due to the coculture with synovial cells, which made possible the creation of a sheet of chondrocytes in a shorter period of time.

2.3. Cell culturing using temperature-responsive culture dishes

The harvested cartilaginous and synovial tissue were finely sliced with scissors and incubated on Petri dishes in DMEM/F12 that contained 0.016% Collagenase Type 1 (Worthington, New Jersey, USA) at 37 °C, 5% CO_2 for 4 h as they were stirred with a stirrer, and the proteins were degraded. Afterwords, the tissue was passed through a cell strainer (BD Falcon™) with a pore size of 100 μm and the cells were retrieved by centrifuge. The chondrocytes were incubated in a culture medium of DMEM/F12 supplemented with 20% fetal bovine serum (FBS; GIBCO, NY, USA) and 1% antibiotics–antimycotic (GIBCO, NY, USA). From day 4 onwards, the culture was maintained by adding a further μg/ml ascorbic acid (Wako Junyakukougyou Corp. Japan), and the synovial cells were maintained in a culture medium of DMEM/F12 supplemented with 10% FBS and 1% antibiotics–antimycotic. All culturing was performed at 37 °C, 5% CO_2 and 95% air. The chondrocytes were seeded on temperature-responsive inserts (5.0 cm^2, CellSeed Inc, Tokyo, Japan) and the synovial cells were seeded in temperature-responsive culture dishes (9.6 cm^2, CellSeed Inc, Tokyo, Japan) and cocultured for 14 days. Both were seeded at a density of 10,000 cells/cm^2.

2.4. Cell sheet retrieval

After the cells were cultured for two weeks, they reached a confluent state and the temperature-responsive inserts were taken out of the incubator and left for 30 min at 25 °C. After the culture medium was removed, polyvinylidene fluoride (PVDF) membranes were used to retrieve the chondrocyte sheets by the method reported by Yamato et al. [37].

Briefly, the PVDF membrane was placed on the cell sheet and then the sheet was rolled up with the membrane from one corner. This method facilitated good retrieval of the cultured chondrocyte sheets. Next, each retrieved cell sheet was placed on top of a new cell sheet and rolled up in the same way to prepare multilayered sheets. This operation was performed 3 times, and triple-layered chondrocyte sheets were fabricated. Because the layered chondrocyte sheets floated in the culture fluid, cell strainers (BD Falcon™) were placed on top of them. The layered chondrocyte sheets were cultured for 1 week. The chondrocytes were continuously cultured for one week in temperature-responsive culture dishes.

2.5. Transplantation of synovial cells and layered chondrocyte sheets

Forty-eight white Japanese rabbits (female, age: 16–18 weeks, weighing: approximately. 3 kg, with each group $n = 4$, six groups) were used in this study. For the surgical procedures we used medetomidine (Domitor 1 mg/ml, Meiji Seika Pharma Co.,Ltd, Tokyo, Japan) delivered by intramuscular injection.

The rabbits were anesthetized using sevoflurane and O_2 gas. After receiving a medial parapatellar incision to one side leg, the patellae were dislocated laterally and an osteochondral defect (diameter: 5 mm; depth: 3 mm) was created on the patellar groove of the femur using a drill and biopsy punch (REF-BP-50F Kai Industries, Seki, Japan). Bleeding from the bone was observed and osteochondral defects were produced. After two week's incubation, once the cells had become confluent, the temperature-responsive culture dish was removed from the incubator and cooled at 25 °C for 30 min. After separation from the culture substrate, the synovial cells were recovered in pellet form and transplanted onto the osteochondral defect. To obtain further coverage of the defect, layered chondrocytes were grafted onto the defect.

The layered chondrocyte sheets and synovial cells were transplanted under the following 6 conditions: Group (A): synovial cells (1.8×10^6) were transplanted, Group (B): only layered chondrocyte sheets (1.7×10^6 cells) were transplanted, Group (C): synovial cells (3.0×10^5) and layered chondrocyte sheets (1.7×10^6 cells) were transplanted on top to cover the osteochondral defects, Group (D): synovial cells (6.0×10^5) and layered chondrocyte sheets (1.7×10^6 cells) were transplanted on top to cover the osteochondral defect, Group (E): synovial cells (1.2×10^6) and layered chondrocyte sheets (1.7×10^6 cells) were transplanted on top to cover the osteochondral defects, Group (F): osteochondral defects only (control group). The synovial cells and layered chondrocyte sheets were transplanted into defects in eight unilateral knees of eight rabbits. After surgery, all of the rabbits were returned to the cage without splinting or immobilization.

2.6. Pain evaluation

One day after transplantation, an Incapacitance Tester (Linton Instrumentation, Norfolk, England) was used to find trends in the weight distribution ratio of the undamaged and damaged limbs, and these trends served as the gauge for evaluating pain. The Incapacitance Tester is a device that facilitates automatic and reproducible pain evaluation by measuring (dual channel weight averaging technique) the weight distribution of both hind limbs. This device is widely used to investigate pain ameliorating effects [38]. In order to habituate the animals to the Incapacitance Tester, each day for 7 days after they were delivered, they were all were placed in the main container (holder) of the device and held still for 5 s. The measurements were performed when the animals were still after they were transferred into the rabbit holder, and when they were still after being removed from and then returned to the holder. This operation was conducted 10 times. The weight distribution of both hind legs was measured 10 times, and the following formula was used to calculate the damaged limb weight distribution ratios (%) obtained by loading the left and right limbs.

$$\text{Damaged limb weight distribution ratio}(\%) = (\text{damaged limb load}(g)/\text{undamaged limb load}(g) + \text{damaged limb load}(g)) \times 100. \quad (1)$$

The average damaged limb weight distribution ratio (%), which was calculated 10 times, was defined as the damaged limb weight distribution ratio (%) per measurement.

After surgery, the measurements were performed a total of 11 times on days 1, 3, 5, 7, 10, 13, 15, 18, 22, 25, and 28.

2.7. Histological evaluation of cartilage repair

We used a total of 48 rabbits, with each group $n = 4$, six groups sacrificed at 4 weeks, and another six at 12 weeks. Rabbits were sacrificed by an overdose of intravenous anesthetic. The results were evaluated and reviewed. The transplanted tissue was removed from the distal portions of the unilateral femurs. It was then fixed in 4% paraformaldehyde for one week. Afterwards, it was decalcified for 2–3 weeks using distilled water (pH: 7.4) containing 10% ethylenediaminetetraacetic acid (EDTA). Next, the tissue was embedded in paraffin waxand sectioned perpendiculary (8 μm sections)through the center of the defect. Each section was stained with safranin O for glycosaminoglycans for histological evaluation.

Immunostaining was performed by the same method as used previously [21,39]. Briefly, deparaffinization was performed using the standard procedure to immunostain the sections. The sections were treated with 0.005% proteinase (type XXIV; Sigma–Aldrich Company, St. Louis, MO, USA) at 37 °C for 30 min. After the sections were washed in PBS (phosphate-buffered saline), they were treated with 0.3% hydrogen peroxide/methanol solution at room temperature for 15–20 min and

endogenous peroxidase was activated. After the sections were washed in PBS, they were reacted for 30 min in a solution containing normal goat serum that had been diluted with PBS at dilution 1:20. Mouse primary monoclonal antibodies, which react with human type I and type II collagen (Daiichi Fine Chemical, Toyama, Japan), were then diluted with PBS containing 1% bovine serum albumin (BSA; Sigma) at dilution 1:200. The sections were left in the solution at 4 °C for one night, then washed 10 times with PBS and reacted at room temperature for 1 h with goat anti-mouse biotin conjugated secondary antibodies that had been diluted with 1% BSA/PBS at dilution 1:100. Afterwards, the sections weres treated for 1 h with horseradish peroxidase and dyed with streptavidin (streptavidin HRP). Finally, they were immersed for 2–4 min in Tris–HCl buffer (pH: 7.6) containing 0.05% diaminobenzidine (DAB) and 0.005% hydrogen peroxide. After immunostaining, the slides were counterstained with Mayer's hematoxylin to increase cell visibility.

In the histological evaluation, scoring was carried out by three single blind examiners, using a modified form of Safranin O as reported by O'Driscoll, Keeley and Salter et al [40], and the International Cartilage Repair Society (ICRS) grading system [24,41].

2.8. Statistical analysis

The analysis of variance (ANOVA) test was used to analyze the rate of loading 28 days after surgery and the histologic appraisals that were performed using the International Cartilage Repair Society (ICRS) grading system. Fisher's test was used for post hoc testing. The results were expressed as the mean ± standard deviation (SD), and $p < 0.05$ was deemed to be a statistically significant difference.

3. Results

3.1. Rate of loading trends

Fig. 1 shows the damaged limb weight distribution ratio (mean ± SD) on days 1, 3, 5, 7, 10, 13, 15, 18, 22, 25 and 28 after graft surgery. Groups (A) to (E) all exhibited an improvement in the damaged limb weight distribution ratio on day 28 compared to immediately after surgery. The results were as follows: Group (A): 34.0 ± 1.6% to 45.2 ± 0.7%; Group (B): 35.6 ± 1.7% to 47.1 ± 0.6%; Group (C): 32.9 ± 3.4% to 48.0 ± 0.3%; Group (D): 35.7 ± 10.1% to 49.1 ± 1.0%; Group (E): 35.6 ± 1.1% to 49.6 ± 0.1%. Conversely, Group (F) exhibited poor damaged limb weight distribution ratio improvement: 33.4 ± 2.9% to 38.8 ± 4.0%. Fig. 2 shows the damaged limb weight distribution ratios on day 28 after surgery. Comparative testing with the ANOVA Test revealed significant differences between Groups (A) to (E) and gGroup (F).

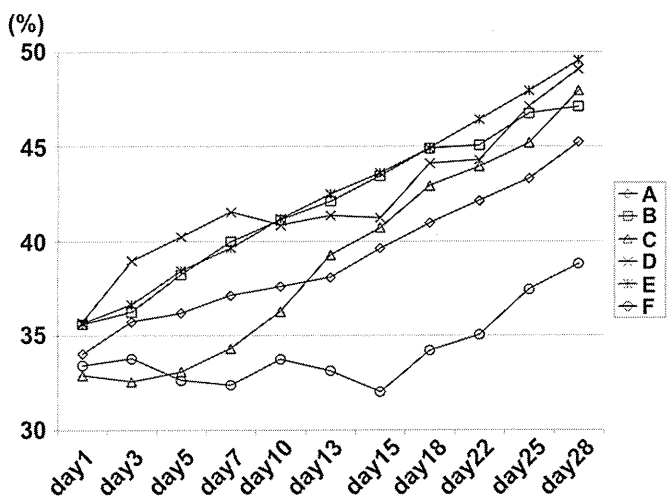

Fig. 1. Damaged limb weight distribution ratio (%) after surgery. Damaged limb weight distribution ratio (%) = (damaged limb load (g)/undamaged limb load (g) + damaged limb load (g)) × 100. The damaged limb weight distribution ratio (mean ± SD) on days 1,3,5,7,10,13,15,18,22,25 and 28 after surgery is shown. Group (A), immediately after surgery, the damaged limb weight distribution ratio of rabbits that received 1.8×10^6 synovial cell transplantation was 34.0 ± 1.6%. However, on day 28 this had improved to 45.2 ± 0.7%. Group (B), the layered chondrocyte sheets (1.7×10^6 cells) transplantation Group improved from 35.6 ± 1.7% to 47.1 ± 0.6%. Group (C), the synovial cell (3.0×10^5 cells) and layered chondrocyte sheets transplantation Group improved from 32.9 ± 3.4% to 48.0 ± 0.3%. Group (D), the synovial cell (6.0×10^5 cells) and layered chondrocyte sheets transplantation Group improved from 35.7 ± 10.1% to 49.1 ± 1.0%. Group (E), the synovial cell (1.2×10^6 cells) and layered chondrocyte sheets transplantation group improved from 35.6 ± 1.1% to 49.6 ± 0.1%. Conversely, osteochondral defect Group (F) exhibited poor damaged limb weight distribution ratio improvement of 33.4 ± 2.9% to 38.8 ± 4.0%.

3.2. Histological evaluation of repair tissue

Operations were uneventful. After surgery, all of the rabbits were returned to the cage and allowed to act freely. We did not find any signs of infection. Four and 12 weeks after surgery, four knees from each group were evaluated.

Fig. 3 shows a histological image of repair tissue that was stained with Safranin-O four and 12 weeks after surgery. Four weeks after surgery, the defects of Groups (A) to (E), the cell graft Groups, had been filled with cartilage-like repair tissue. However, we observed that in Group (F), some defects had not been filled with repair tissue. In Group (A),we observed that the implants had been partially replaced with fibrous tissue. Integration with the surrounding cartilage was good. At that time, formation of subchondral bone, including hypertrophic chondrocytes, was inadequate in the lower portion of the implants. In Group (B), Safranin-O staining revealed irregular thickness of the superficial cartilage layer. Integration with the surrounding cartilage was good. Subchondral bone formation was inadequate. In Group (C), Safranin-O staining revealed that integration with surrounding normal cartilage was also good. Although the superficial layer also included some hypertrophic chondrocytes, smooth convex repair was achieved. Similarly, in the case of Groups (D) and (E), Safranin-O staining revealed convex repair tissue formation, and structural consistency, defect filling rates and the condition of the superficial layer of the defect also tended to be better than the other Groups.

Even 12 weeks after transplantation surgery, the defects of Groups (A) to (E), the cell transplantation Groups, had been filled with cartilage-like repair tissue. No cartilage layer was observed in

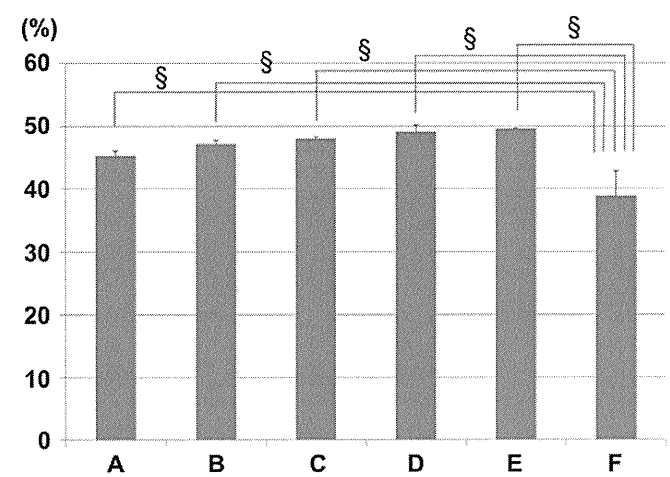

Fig. 2. At 28 days after surgery, a damaged limb weight distribution ratio of ($p < 0.05$, §) was deemed significant. VS Group (F). The damaged limb weight distribution ratio on day 28 after surgery is shown. Group (A), the damaged limb weight distribution ratio of rabbits that received 1.8×10^6 synovial cell transplantation was 45.2 ± 0.7%. Group (B), the layered chondrocyte sheets (1.7×10^6 cells) transplantation Group: 47.1 ± 0.6%. Group (C), the synovial cell (3.0×10^5 cells) and layered chondrocyte sheets transplantation Group: 48.0 ± 0.3%. Group (D), the synovial cell (6.0×10^5 cells) and layered chondrocyte sheets transplantation Group: 49.1 ± 1.0%. Group (E), the synovial cell (1.2×10^6 cells) and layered chondrocyte sheets transplantation Group: 49.6 ± 0.1%. Group (F), the osteochondral defect Group: 38.8 ± 4.0%. Significant differences were observed between Groups (A) to (E) and Group (F).

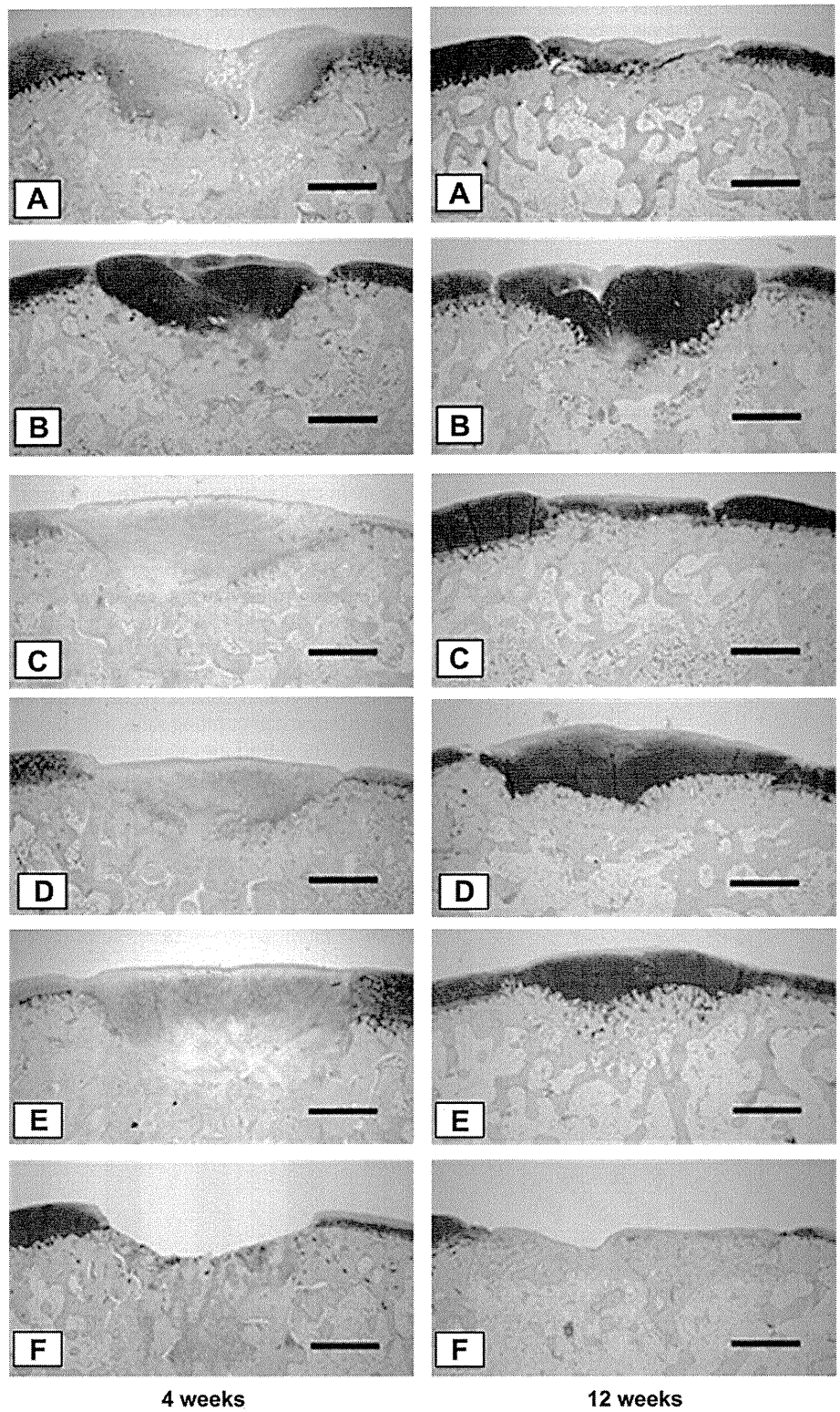
A
A
B
B
C
C
D
D
E
E
F
F
4 weeks
12 weeks

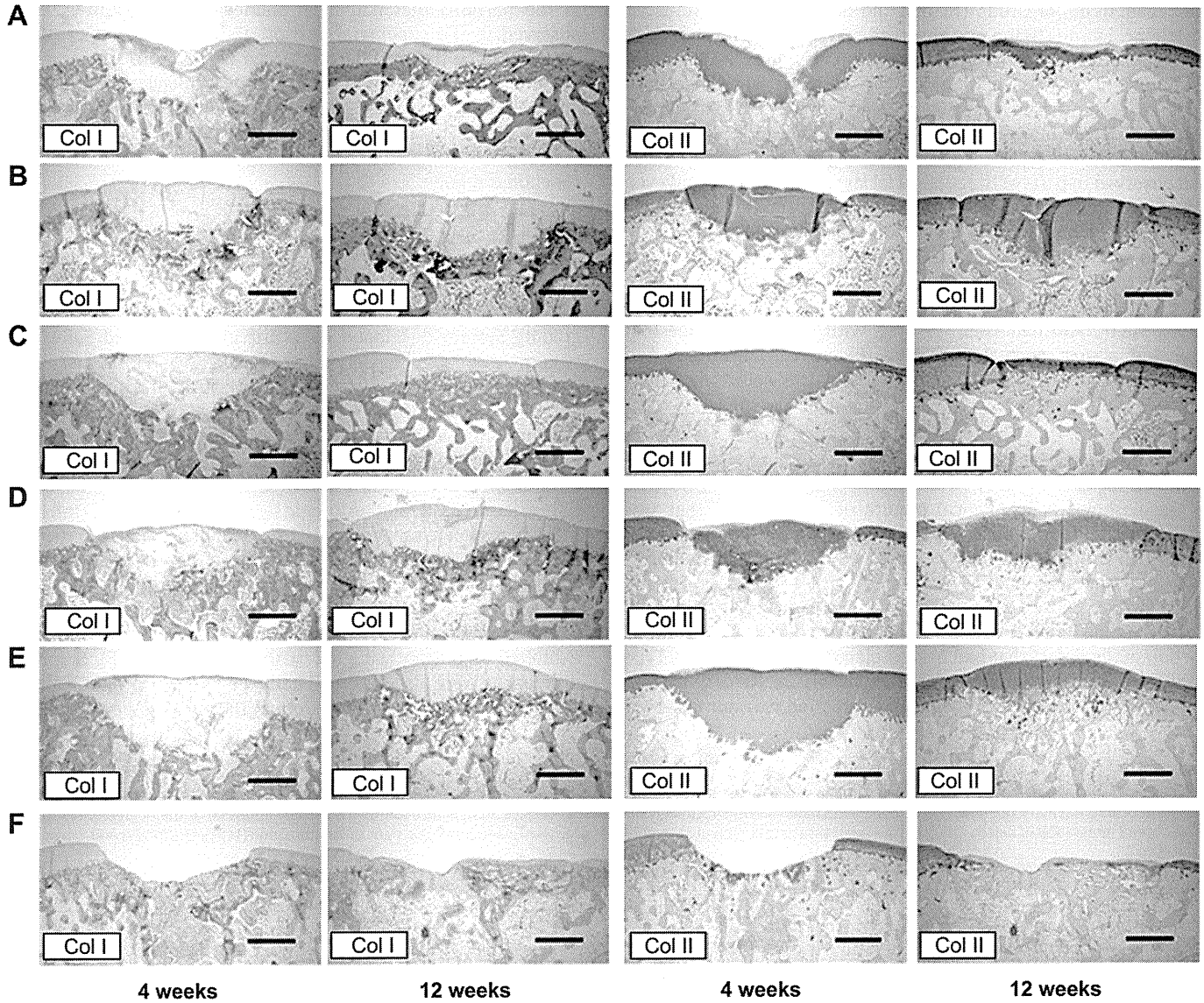

Fig. 4. Histological picture of repair tissue that was immunostained four and 12 weeks after surgery. (Bar = 1000 μm). Group (A): 1.8×10^6 synovial cells were transplanted. Group (B): only layered chondrocyte sheets (1.7×10^6 cells) were transplanted. Group (C): 3.0×10^5 synovial cells and layered chondrocyte sheets 1.7×10^6 synovial cells were transplanted on top to cover the osteochondral defects. Group (D): 6.0×10^5 synovial cells and layered chondrocyte sheets 1.7×10^6 cells were transplanted on top to cover the osteochondral defects. Group (E): 1.2×10^6 synovial cells were and layered chondrocyte sheets (1.7×10^6 cells) were transplanted on top to cover the osteochondral defects. Group (F): osteochondral defects only (control Group). Immunostaining was performed with type I (Col I) and type II (Col II) collagen, and the results were evaluated and reviewed. Four weeks after surgery, In Groups (A) to (E), type II collagen expression was observed in implant tissue that had been stained with Safranin-O, it was expressed uniformly in the surrounding cells. Type II collagen made the cartilaginous repair tissue borders clearer. Conversely, although type I collagen expression was not observed in the portions that had been stained with Safranin-O, it was observed in the superficial portion and superficial layer of subchondral bone that had been replaced with fibrous tissue. Twelve weeks after surgery, Similarly, in Groups (A) to (E), type II collagen expression was observed in the implant tissue and pericellular normal cartilage, and type I collagen expression was observed in the superficial portion of fibrocartilage and the superficial layer of subchondral bone.

Fig. 3. Histologic findings for repair tissue that was stained with Safranin-O four and 12 weeks after surgery (Bar = 1000 μm). In Group (A), Safranin-O staining was performed on the group that received 1.8×10^6 synovial cell transplantation. Four weeks after surgery, however, we observed that the implants had been partially replaced with fibrous tissue. At that time, formation of subchondral bone, including hypertrophic chondrocytes, was inadequate in the lower portion of the graft tissue. Twelve weeks after surgery, the defect had been filled with cartilage-like repair tissue. Although fibrous tissue was observed in the superficial portion, subchondral bone formation was good. In Group (B), four weeks after surgery, Safranin-O staining performed on the Group that received layered chondrocyte sheets (1.7×10^6 cells) transplantation revealed that integration with the surrounding cartilage was good. Subchondral bone formation was inadequate. Twelve weeks after surgery, fibrous tissue was observed in portions sof the superficial layer of repair tissue that were stained with Safranin-O. However, defect filling rates, subchondral bone and integration with the surrounding cartilage layer were good. In Group (C), synovial cells (3.0×10^5) and layered chondrocyte sheets (1.7×10^6 cells) transplanted on top to cover the osteochondral defects. Four weeks after surgery, integration with the surrounding normal cartilage was good. Although the superficial layer also included some hypertrophic chondrocytes, smooth convex repair was achieved. Twelve weeks after surgery, fibrous tissue was observed in the superficial portion; however, Safranin-O stainability and subchondral bone formation were good. In Group (D), synovial cells (6.0×10^5) and layered chondrocyte sheets (1.7×10^6 cells) transplanted on top to cover the osteochondral defects. Four weeks after surgery, the formation of convex repair tissue was achieved, and structural consistency, defect filling rates and condition of the superficial layer of the defect were good. Twelve weeks after surgery, the cartilage layer exhibited a columnar arrangement, and good repair was achieved. In Group (E), 1.2×10^6 cells and layered chondrocyte sheets (1.7×10^6) transplanted on top to cover the osteochondral defects. Four weeks after surgery, similarly, the formation of convex repair tissue (stained with Safranin-O) was achieved, and structural consistency, defect filling rates and condition of the superficial layer of the defect were good. Twelve weeks after surgery, Similarly, the condition of the implants tissue, tissue filling rates and subchondral bone formation were all good, and the transplant cartilage layer exhibited a columnar arrangement and had been repaired with hyaline cartilage that appeared almost normal. In Group (F), osteochondral defects only (control Group). Four weeks after surgery, we observed that the defects had not been filled with repair tissue. Twelve weeks after surgery, the implant tissue exhibited no cartilage layer, and had not been replaced with bone.

the repair tissue of Group (F), and the defect had been replaced with bone. Fibrous tissue was observed in the superficial portion of Group (A) but subchondral bone formation was good. In the case of Group (B), fibrous tissue was observed in parts of the superficial layer of repair tissue that had been stained with Safranin-O; however, defect filling rates, subchondral bone and integration with the surrounding cartilage layer were good. Fibrous tissue was also observed in parts of the superficial layer of Group (C); however, Safranin-O stainability and subchondral bone formation were good. In Group (D), the cartilage layer exhibited a columnar arrangement, and good repair was achieved. In Group (E), the condition of the graft tissue, defect filling rates and subchondral bone formation were all good. The graft cartilage layer exhibited a columnar arrangement, and had been repaired with hyaline cartilage that appeared almost normal. In Group (F), no cartilage layer had formed in the transplantation tissue, and the defect had been replaced with bone.

3.3. Immunohistochemical evaluation

Fig. 4 shows a histological picture of repair tissue that was immunostained four and 12 weeks after surgery. Four weeks after surgery, In Groups (A) to (E), we observed type II collagen expression in tissue that had been stained with Safranin-O. Type II collagen was expressed uniformly in the surrounding cells. In Group (A), no type II collagen expression was observed in the portion of the defect that had been replaced by fibrous tissue. Type II collagen made the cartilaginous repair tissue borders clearer. Conversely, although type I collagen expression was not observed in the portions that had been stained with Safranin-O, it was observed in the superficial portion and superficial layer of subchondral bone that had been replaced with fibrous tissue.

Similarly, 12 weeks after surgery, type II collagen expression was observed in the grafted tissue and pericellular normal cartilage of groups (A) to (E), and type I collagen expression was observed in the superficial portion of fibrocartilage and the superficial layer of subchondral bone.

3.4. Histological scoring of repair tissue

We evaluated the repair tissue using the ICRS histological grading system [24,40,41] (Table 1), which is a modification of the grading system developed by O'Driscoll, Keeley and Salter. This system evaluates repair tissue based on 11 items: tissue morphology (Ti); matrix staining (Matx); structural integrity (Stru); cluster formation (Clus); tidemark opening (Tide); bone formation (Bform); histologic appraisal of surface architecture (SurfH); histologic appraisal of the degree of defect filling (FilH); lateral integration of defect-filling tissue (Latl); basal integration of defect-filling tissue (Basl); and histologic signs of inflammation (InfH). The total scores range ranged from 11 to 45. Table 2 and Fig. 5 show the ICRS grading system results four weeks after surgery. Four weeks after surgery, the results were as follows: Group (A): 26.8 ± 3.8; Group (B): 25.0 ± 6.2; Group (C): 30.5 ± 3.8; Group (D): 35.0 ± 4.2; Group (E): 35.8 ± 3.8; Group (F): 17.0 ± 1.2. Groups (A) to (E) exhibited significantly higher scores than Group (F). Significant differences were also observed between Group (A) and Groups (D) and (E), and Group (B) and Groups (D) and (E). Viewed by item,

Table 1
ICRS Histological grading system. This system evaluates repair tissue based on 11 items: tissue morphology (Ti); matrix staining (Matx); structural integrity (Stru); cluster formation (Clus); tidemark opening (Tide); bone formation (Bform); histologic appraisal of surface architecture (SurfH); histologic appraisal of the degree of defect filling (FilH); lateral integration of defect-filling tissue (Latl); basal integration of defect-filling tissue (Basl); and histologic signs of inflammation (InfH). The total scores range ranged from 11 to 45.

Ti	**Tide**	**Latl**
Tissue morphology	Intactness of the calcified cartilage layer, formation of tidemark	Lateral integration of implanted material
4: mostly hyaline cartilage	1: <25% of the calcified cartilage layer intact	1: not bonded
3: mostly fibrocartilage	2: 25–49% of the calcified cartilage layer intact	2: bonded at one end/partially both ends
2: mostly non-cartilage	3: 50–75% of the calcified cartilage layer intact	3: bonded at both sides
1: exclusively non-cartilage	4: 76–90% of the calcified cartilage layer intact	
	5: complete intactness of the calcified cartilage layer	
Matx	**Bform**	**Basl**
Matrix staining	Subchondral bone formation	Basal integration of implanted material
1: none	1: no formation	1: <50%
2: slight	2: slight	2: 50–70%
3: moderate	3: strong	3: 70–90%
4: strong		4: 91–100%
Stru	**SurfH**	InfH
Structural integrity	Histologic appraisal of surface architecture	Inflammation
1: severe disintegration	1: severe fibrillation or disruption	1: no inflammation
2: cysts or disruptions	2: moderate fibrillation or irregularity	3: slight inflammation
3: no organization of chondrocytes	3: slight fibrillation or irregularity	5: strong inflammation
4: beginning of columnar organization of chondrocytes	4: normal	
5: normal, similar to healthy mature cartilage		
Clus	**FilH**	**Hgtot**
Chondrocyte clustering in implant	Histologic appraisal defect filling	Histological grading system
1: 25–100% of the cells clustered	1: <25%	Some of the histologic variables:
2: <25% of the cells clustered	2: 26–50%	tissue morphology(Ti),
3: no clusters	3: 51–75%	matrix staining (Matx), structural integrity (Stru),
	4: 76–90%	cluster formation (Clus), tidemark opening (Tide),
	5: 91–110%	bone formation (Bform), histologic surface architecture (SurfH),
		histologic degree of defect filling (FilH),
		lateral integration of defect-filling tissue (Latl),
		basal integration of defect-filling tissue (Basl),
		and histologic signs of inflammation (InfH)
		Maximum total: 45 points

Table 2
ICRS grading system 4W; values are the mean ± SD. The total score range is from 11 (no repair) to 45 (normal articular cartilage). Group (A): 1.8×10^6 synovial cells were transplanted. Group (B): only layered chondrocyte sheets (1.7×10^6 cells) were transplanted. Group (C): 3.0×10^5 synovial cells and layered chondrocyte sheets (1.7×10^6 cells) were transplanted on top to cover the osteochondral defects. Group (D): 6.0×10^5 synovial cells and layered chondrocyte sheets (1.7×10^6 cells) were transplanted on top to cover the osteochondral defects. Group (E): 1.2×10^6 synovial cells and layered chondrocyte sheets (1.7×10^6 cells) were transplanted on top to cover the osteochondral defects. Group (F): osteochondral defects only (control Group). Four weeks after graft surgery, histologic appraisals were performed using the ICRS grading system. The results were as follows: Group (A): 26.8 ± 3.8; Group (B): 25.0 ± 6.2; Group (C): 30.5 ± 3.8; Group (D): 35.0 ± 4.2; Group (E): 35.8 ± 3.8; Group (F): 17.0 ± 1.2. Viewed by item, Groups (A) to (E) exhibited significantly higher Matx, FilH, and Basl scores than Group (F), while Groups (D) and (E) exhibited significantly higher Clus and Tide scores than Groups (A) and (B).

	A	B	C	D	E	F
Ti	2.50 ± 0.6	2.25 ± 0.5	3.00 ± 0.0	3.00 ± 0.8	3.25 ± 0.5	1.50 ± 0.6
Matx	1.25 ± 0.5	2.00 ± 0.8	2.50 ± 0.6	3.00 ± 0.8	2.75 ± 0.5	1.00 ± 0.0
Stru	2.75 ± 1.0	2.50 ± 1.0	3.50 ± 0.6	3.75 ± 0.5	3.75 ± 0.5	2.00 ± 0.0
Clus	1.50 ± 0.6	1.25 ± 0.5	1.50 ± 0.6	2.00 ± 0.0	2.00 ± 0.0	1.00 ± 0.0
Tide	1.25 ± 0.5	1.50 ± 1.0	2.00 ± 0.8	3.25 ± 0.5	3.50 ± 1.0	1.00 ± 0.0
Bform	1.75 ± 0.5	2.00 ± 0.0	2.25 ± 0.5	2.25 ± 0.5	2.50 ± 0.6	1.50 ± 0.6
SurfH	1.75 ± 0.6	2.00 ± 0.8	1.50 ± 0.6	2.25 ± 0.5	2.25 ± 0.5	1.00 ± 0.0
FilH	3.00 ± 0.8	2.25 ± 1.3	3.50 ± 1.3	4.00 ± 0.8	4.00 ± 1.4	1.00 ± 0.0
Latl	2.50 ± 1.0	1.50 ± 0.6	2.25 ± 0.5	2.75 ± 0.5	2.75 ± 0.5	1.00 ± 0.0
Basl	3.50 ± 0.6	2.75 ± 0.5	3.50 ± 0.6	3.75 ± 0.5	4.00 ± 0.0	1.00 ± 0.0
InfH	5.00 ± 0.0	5.00 ± 0.0	5.00 ± 0.0	5.00 ± 0.0	5.00 ± 0.0	5.00 ± 0.0
Hgtot	26.8 ± 3.8	25.0 ± 6.2	30.5 ± 3.8	35.0 ± 4.2	35.8 ± 3.8	17.0 ± 1.2

Table 3
ICRS grading system 12W, Values are the mean ± SD. The total score range is from 11 (no repair) to 45 (normal articular cartilage). Group (A): 1.8×10^6 synovial cells were transplanted. Group (B): only layered chondrocyte sheets (1.7×10^6 cells) were transplanted. Group (C): 3.0×10^5 synovial cells and layered chondrocyte sheets (1.7×10^6 cells) were transplanted on top to cover the osteochondral defects. Group (D): 6.0×10^5 synovial cells and layered chondrocyte sheets (1.7×10^6 cells) were on top to cover the osteochondral defects. Group (E): 1.2×10^6 synovial cells and layered chondrocyte sheets (1.7×10^6 cells) were transplanted on top to cover the osteochondral defects. Group (F): osteochondral defects only (control group). Twelve weeks after surgery, histologic appraisals were performed using the ICRS grading system. Group (A): 29.0 ± 0.8; Group (B): 31.8 ± 5.4; Group (C): 32.3 ± 5.0; Group (D): 38.8 ± 2.1; Group (E): 40.1 ± 2.5; Group (F): 23.3 ± 2.4. Viewed by item, Groups (A) to (E) exhibited significantly higher Matx and InfH scores than Group (F), while Groups (D) and (E) exhibited significantly higher SurfH, FilH and Tide scores than Groups (A) and (B).

	A	B	C	D	E	F
Ti	2.00 ± 0.8	2.50 ± 1.3	2.75 ± 1.5	3.25 ± 1.0	3.75 ± 0.5	1.75 ± 0.5
Matx	2.50 ± 0.6	2.25 ± 0.5	2.50 ± 0.6	3.25 ± 0.5	3.50 ± 0.6	1.25 ± 0.5
Stru	2.50 ± 0.6	3.25 ± 1.0	3.25 ± 1.0	3.75 ± 0.5	4.25 ± 0.5	2.25 ± 0.5
Clus	2.00 ± 0.0	3.00 ± 0.0	2.75 ± 0.5	3.00 ± 0.0	3.00 ± 0.0	1.75 ± 0.5
Tide	2.25 ± 0.5	2.00 ± 0.8	2.00 ± 1.4	3.75 ± 0.5	4.25 ± 0.5	1.25 ± 0.5
Bform	2.25 ± 0.5	1.75 ± 1.0	2.00 ± 1.2	3.00 ± 0.0	2.25 ± 0.5	1.75 ± 1.0
SurfH	2.00 ± 0.0	1.50 ± 0.6	2.25 ± 0.5	2.75 ± 0.5	2.75 ± 0.5	1.00 ± 0.0
FilH	3.25 ± 0.5	3.75 ± 0.5	4.25 ± 0.5	4.50 ± 0.6	5.00 ± 0.0	3.50 ± 0.6
Latl	2.25 ± 0.5	2.75 ± 0.5	2.25 ± 1.0	2.50 ± 0.6	3.00 ± 0.0	1.75 ± 1.0
Basl	3.50 ± 0.6	4.00 ± 0.0	3.25 ± 1.0	4.00 ± 0.0	4.00 ± 0.0	3.50 ± 0.6
InfH	4.50 ± 1.0	5.00 ± 0.0	5.00 ± 0.0	5.00 ± 0.0	5.00 ± 0.0	3.50 ± 1.0
Hgtot	29.0 ± 0.8	31.8 ± 5.4	32.3 ± 5.0	38.8 ± 2.1	40.8 ± 2.5	23.3 ± 2.4

Groups (A) to (E) exhibited significantly higher Matx, FilH, and Basl scores than Group (F), while Groups (D) and (E) exhibited significantly higher Clus and Tide scores than Group (B).

Table 3 and Fig. 6 show the ICRS grading system results 12 weeks after surgery. Group (A): 29.0 ± 0.8; Group (B) Group: 31.8 ± 5.4; Group (C): 32.3 ± 5.0; Group (D): 38.8 ± 2.1; Group (E): 40.8 ± 2.5; Group (F): 23.3 ± 2.4. Similarly, four weeks after surgery, Groups (A) to (E) exhibited significantly higher scores than Group (F), and significant differences were observed between Group (A) and Groups (D) and (E) and Group (B) and Groups (D) and (E). At 12 weeks, significant differences were also observed between Group (C) and Groups (D) and (E). Viewed by item, Groups (A) to (E) exhibited significantly higher Matx and InfH scores than Group (F), while Groups (D) and (E) exhibited significantly higher SurfH, FilH and Tide scores than Groups (A) and (B).

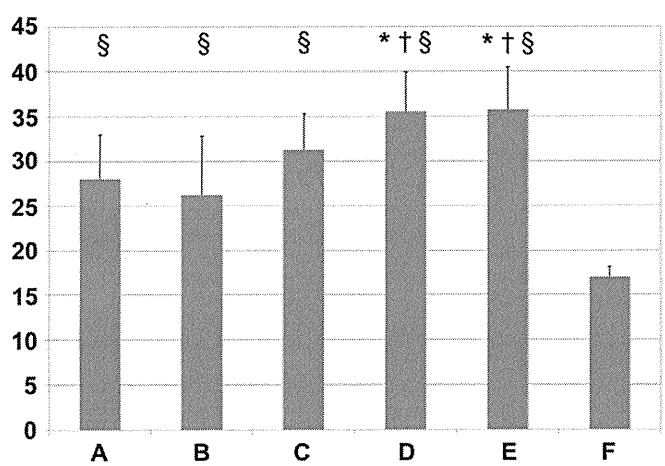

Fig. 5. ICRS grading system 4W, ($p < 0.05$) was deemed significant. (§) VS Group (F), (*) VS Group (A), (†) VS Group (B). Group (A): 1.8×10^6 synovial cells were transplanted. Group (B): only layered chondrocyte sheets (1.7×10^6 cells) were transplanted. Group (C): 3.0×10^5 synovial cells and layered chondrocyte sheets (1.7×10^6 cells) were transplanted on top to cover the osteochondral defects. Group (D): 6.0×10^5 synovial cells and layered chondrocyte sheets (1.7×10^6 cells) were transplanted on top to cover the osteochondral defects. Group (E): 1.2×10^6 synovial cells and layered chondrocyte sheets (1.7×10^6 cells) were transplanted on top to cover the osteochondral defects. Group (F): osteochondral defects only (control Group). Four weeks after surgery, histologic appraisals were performed using the ICRS grading system. Groups (A) to (E) exhibited significantly higher scores than Group (F). Significant differences were observed between Group (A) and Groups (D) and (E), and Group (B) and Groups (D) and (E).

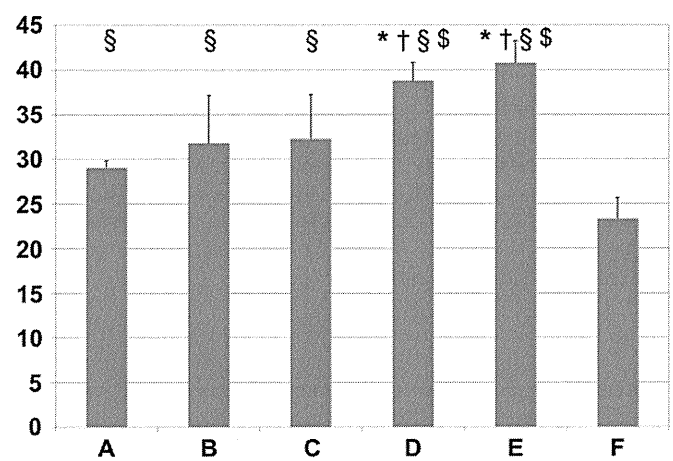

Fig. 6. ICRS grading system 12W, ($P < 0.05$) was deemed significant. (§) VS Group (F), (*) VS Group (A), (†) VS Group (B), ($) VS Group (C). Group (A): 1.8×10^6 synovial cells were transplanted. Group (B): only layered chondrocyte sheets (1.7×10^6 cells) were transplanted. Group (C): 3.0×10^5 synovial cells and layered chondrocyte sheets (1.7×10^6 cells) were transplanted on top to cover the osteochondral defects. Group (D): 6.0×10^5 synovial cells and layered chondrocyte sheets (1.7×10^6 cells) were transplanted on top to cover the osteochondral defects. Group (E): 1.2×10^6 synovial cells and layered chondrocyte sheets (1.7×10^6 cells) were transplanted on top to cover the osteochondral defects. Group (F): osteochondral defects only (control Group). Twelve weeks after surgery, histologic appraisals were performed using the ICRS grading system. Similarly, four weeks after surgery, Groups (A) to (E) exhibited significantly higher scores than Group (F), and significant differences were observed between Group (A) and Groups (D) and (E), and Group (B) and Groups (D) and (E). At 12 weeks, significant differences were also observed between Group (C) and Groups (D) and (E).

4. Discussion

In recent years, there has been widespread use of cell grafts to repair articular cartilage, both in animal experiments [15,17,18,21–25] and in clinical application [11–14,16,19,20]. Ochi et al have reported that better results have been obtained using grafts of tissue-engineered cartilage than chondrocytes, and have obtained good results in clinical application using tissue-engineered cartilage grafts embedded in atelocollagen gel [42]. Generally speaking, scaffolds consist of synthetic polymers or biological materials, and therefore, there are numerous concerns regarding their long-term biocompatibility [18]. In order to eliminate these unknown risks, it would be ideal not to use scaffolds. From this perspective, scaffold free cell grafts would be an excellent option. Mainil-Varlet P et al. produced scaffold free tissue-engineered cartilage using a static bioreactor system [23]. Nagai et al. produced tissue-engineered cartilage using a rotation culture method and a lower cell count (6.0×10^6 cells) [22]. Synovial cell grafts are widely used to repair articular cartilage defects. Hunziker et al have reported synovial cells played an important role in the repair of the cartilage defects [43]. Koga et al have reported good results from creating osteochondral defects in rabbit knees and then grafting synovium-derived MSCs used in conjunction with periosteum [44]. Ando et al have reported the inclusion of fibrous tissue in repaired tissue after investigating articular cartilage repair using synovial cells [33]. The current study sought to repair articular cartilage through the combined use of layered chondrocyte sheets and synovial cells, aiming for completely hyaline cartilage repair by solving the problem of fibrous tissue inclusion.Previously, Kaneshiro et al. reported that layered chondrocyte sheets have an inhibiting effect on cartilage degeneration using cartilage partial-thickness defect models [31], and Ebihara et al. reported good effects from treatment with layered chondrocyte sheets using minipig osteochondral defect models; however, they reported that in some cases, subchondral bone formation was inadequate [36]. It has been reported that layered chondrocyte sheets may be excellent cell grafts that are scaffold free and possess a three-dimensional structure; in this study, we investigated articular cartilage repair by combining layered chondrocyte sheets with synovial cells in an effort to achieve a better tissue-like structure.

Four weeks after surgery, the transplanted cell groups improved significantly compared to the control groups, which suggests that the cell implants were effective at ameliorating pain. This implies that the synovial cell or chondrocyte sheet implants repaired the articular cartilage defects, improving the defects to the point that they could withstand loading.

In the histologic appraisal, significant differences between groups (A) to (E) and group (F) were observed four and 12 weeks after surgery, suggesting that cell transplantation contribute more to tissue repair than non-cell implants. Furthermore, significant differences were observed between groups (A) and (B) and groups (D) and (E), which suggests that the combination of layered chondrocyte sheets with synovial cell transplantation was effective.

Ando et al. investigated articular cartilage repair using synovial cell implants and found that the superficial portion contained fibrous tissue. Therefore, they reported that synovial cell implants might promote chondrogenic differentiation *in vivo* [33]. From the perspective of implant cell counts, the synovial cell counts we employed (group (A): 1.8×10^6 cells (C):3.0×10^5 cells (D):6.0×10^5 cells (E):1.2×10^6 cells) were clearly lower than ACI reports [44] which used other synovial cells.

In this study, we achieved good repair by combining synovial cell transplantation with layered chondrocyte sheets, even though only few synovial cell implants were used. Nevertheless, although no significant differences between group (A) and groups (B) and (C) or group (C) and groups (D) and (E) were observed four weeks after surgery, significant differences between group (C) and groups (D) and (E) were observed 12 weeks after surgery. These results indicate that if it transplants only synovial cells which may be insufficient, and layered chondrocyte sheets and synovial cells will be combined and transplanted into osteochondral defects, the grafting of 6.0×10^5 or more synovial cells may be beneficial. In the future, further study will be required to optimize the implant cell count given factors that include varying states of repair, knee joint volume and osteochondral defect size depending on the animal species. This report suggests that a combination of layered chondrocyte sheets and synovial cells may be effective in repairing articular cartilage.

5. Conclusions

In rabbit osteochondral defect models, pain alleviating effects and better tissue repair were achieved by combining layered chondrocyte sheets with synovial cells transplantations. The condition of Group (E): synovial cells (1.2×10^6) and layered chondrocyte sheets (1.7×10^6 cells) demonstrated excellent results of both defect filling rates and subchondral bone formation. The graft cartilage layer exhibited a columnar arrangement, and had been repaired with hyaline cartilage. Transplantation conditions and other factors must therefore be further investigated.

References

[1] Paget J. Healing of cartilage. Clin Orthop 1969;64:7–8.
[2] Steadman J, Rodkey W, Rodrigo J. Microfracture: surgical technique and rehabilitation to treat chondral defects. Clin Orthop Relat Res 2001;391(Suppl 1): 362–9.
[3] Steadman J, Rodkey W, Briggs K. Microfracture to treat full-thickness chondral defects: surgical technique, rehabilitation, and outcomes. J Knee Surg 2002; 15:170–6.
[4] Mithoefer K, Williams 3rd RJ, Warren RF, Potter HG, Spock CR, Jones EC, et al. Chondral resurfacing of articular cartilage defects in the knee with the microfracture technique. Surgical technique. J Bone Joint Surg Am 2006;88:294–304.
[5] Hangody L, Kish G, Karpati Z, Udvarhelyi I, Szerb I, Bely M. Autogenous osteochondral graft technique for replacing knee cartilage defects in dogs. Orthopedics 1997;5:175–81.
[6] Hangody L, Feczko P, Bartha L, Bodo G, Kish G. Mosaicplasty for the treatment of articular defects of the knee and ankle. Clin Orthop Relat Res 2001;391-(Suppl):328–36.
[7] Szerb I, Hangody L, Duska Z, Kaposi NP. Mosaicplasty: long-term follow-up. Bull Hosp Jt Dis 2005;63:54–62.
[8] Solchaga LA, Yoo JU, Lundberg M, Dennis JE, Huibregtse BA, Goldberg VM, et al. Hyaluronan-based polymers in the treatment of osteochondral defects. J Orthop Res 2000;18:773–80.
[9] Caplan AI, Elyaderani M, Mochizuki Y, Wakitani S, Goldberg VM. Principles of cartilage repair and regeneration. Clin Orthop Relat Res 1997;342:254–72.
[10] Shapiro F, Koide S, Glimcher MJ. Cell origin and differentiation in the repair of full-thickness defects of articular cartilage. J Bone Joint Surg Am 1993;75: 532–53.
[11] Brittberg M, Lindahl A, Nilsson A, Ohlsson C, Isaksson O, Peterson L. Treatment of deep cartilage defects knee with autologus chondrocyte transplantation. N Engl J Med 1994;331:889–95.
[12] Peterson L, Minas T, Brittberg M, Lindahl A. Treatment of osteochondritis dissecans of the knee with autologouschondrocyte transplantation: results at two to ten years. J Bone Joint Surg Am 2003;85-A(Suppl 2):17–24.
[13] Zaslav K, Cole B, Brewster R, DeBerardino T, Farr J, Fowler P, et al. A prospective study of autologous chondrocyte implantation in patients with failed prior treatment for articular cartilage defects of the knee: results of the Study of the Treatment of Articular Repair (STAR) clinical trial. Am J Sports Med 2009;37:42–55.
[14] Moseley Jr JB, Anderson AF, Browne JE, Mandelbaum BR, Micheli LJ, Fu F, et al. Long-term durability of autologus chondrocyte implantation: a multicenter, observational study in US patients. Am J Sports Med 2010;38:238–46.
[15] Darling EM, Athanasiou KA. Articular cartilage bioreactor and bioprocess. Tissue Eng 2003;9:9–26.
[16] Backwalter JA, Lohmander S. Current concepts review. Operative treatment of osteoarthritis. Current practice and future development. J Bone Joint Surg Am 1994;76:1405–18.
[17] Freed LE, Grande DA, Lingbin Z, Emmanual J, Marquis JC, Langer R. Joint resurfacing using allograft chondrocytes and synthetic biodegradable polymer scaffolds. J Biomed Mater Res 1994;28:891–9.

[18] Hunziker EB. Articular cartilage repair: basic science and clinical progress. A review of the current status and prospects. Osteoarthr Cartil 2001;10:432–63.
[19] Marcacci M, Berruto M, Brocchetta D, Delcogliano A, Ghinelli D, Gobbi A, et al. Articular cartilage engineering with Hyalograft C: 3-year clinical results. Clin Orthop Relat Res 2005;435:96–105.
[20] Crawford DC, Heveran CM, Cannon Jr WD, Foo LF, Potter HG. An autologus cartilage tissue implant NeoCart for treatment of grade III chondral injury to the distal femur: prospective clinical safety trial at 2 years. Am J Sports Med 2009;39:1334–43.
[21] Nagai T, Sato M, Furukawa KS, Kutsuna T, Ohta N, Ushida T, et al. Optimization of allograft implantation using scaffold-free chondrocyte plates. Tissue Eng Part A 2008;14:1225–35.
[22] Nagai T, Furukawa KS, Sato M, Ushida T, Mochida J. Characteristics of a scaffold-free articular chondrocyte plate grown in rotational culture. Tissue Eng Part A 2008;14:1183–93.
[23] Mainil-Varlet P, Rieser F, Grogan S, Mueller W, Saager C, Jakob RP. Articular cartilage repair using a tissue-engineered cartilage-like implant: an animal study. Osteoarthr Cartil 2001;9:S6–15.
[24] Brehm W, Aklin B, Yamashita T, Rieser F, Trub T, Jakob RP, et al. Repair of superficial osteochondral defects with an autologous scaffold-free cartilage construct in a caprine model: implantation method and short-term results. Osteoarthr Cartil 2006;14:1214–26.
[25] Park K, Huang J, Azar F, Jin RL, Min BH, Han DK, et al. Scaffold-free, engineered porcine cartilage construct for cartilage defect repair—in vitro and in vivo study. Artif Organs 2006;30:586–96.
[26] Okano T, Yamada N, Okuhara M, Sakai H, Sakurai Y. Mechanism of cell detachment from temperature-modulated, hydrophilic–hydrophobic polymer surfaces. Biomaterials 1995;16:297–303.
[27] Okano T, Yamada N, Sakai H, Sakurai Y. A novel recovery system for cultured cells using plasma-treated polystyrene dishes grafted with poly(N-isopropylacrylamide). J Biomed Mater Res 1993;27:1243–51.
[28] Shimizu T, Yamato M, Akutsu T, Shibata T, Isoi Y, Kikuchi A, et al. Electrically communicating three-dimensional cardiac tissue mimic fabricated by layered cultured cardiomyocyte sheets. J Biomed Mater Res 2002;60:110–7.
[29] Nishida K, Yamato M, Hayashida Y, Watanabe K, Maeda N, Watanabe H, et al. Functional bioengineered corneal epithelial sheet grafts from corneal stem cells expanded ex vivo on a temperature-responsive cell culture surface. Transplantation 2004;77:379–85.
[30] Nishida K, Yamato M, Hayashida Y, Watanabe K, Yamamoto K, Adachi E, et al. Corneal reconstruction with tissue-engineered cell sheets composed of autologous oral mucosal epithelium. N.Engl J Med 2004;351:1187–96.
[31] Kaneshiro N, Sato M, Ishihara M, Mitani G, Sakai H, Mochida J. Bioengineered chondrocyte sheets may be potentially useful for the treatment of partial thickness defects of articular cartilage. Biochem Biophys Res Commun 2006; 349:723–31.
[32] Mitani G, Sato M, Jeong I, Lee K, Kaneshiro N, Ishihara M, et al. The properties of bioengineered chondrocyte sheets for cartilage regeneration. BMC Biotechnol 2009;9:17.
[33] Ando W, Tateishi K, Hart DA, Katakai D, Tanaka Y, Nakamura N, et al. Cartilage repair using an in vitro generated scaffold-free tissue-engineered construct derived from porcine synovial mesenchymal stem cell. Biomaterials 2007;28: 5462–70.
[34] Sekiya S, Shimizu T, Yamato M, Kikuchi A, Okano T. Bioengineered cardiac cell sheet grafts have intrinsic angiogenic potential. Biochem Biophys Res Commun 2006;341:573–82.
[35] Huch K, Stooe J, Gunther KP, Puhl W. Interactions between human osteoarthritic chondrocytes and synovial fibroblasts in co-culture. Clin Exp Rheumatol 2001;19:27–33.
[36] Ebihara G, Sato M, Yamato M, Mitani G, Kutsuna T, Nagai T, et al. Cartilage repair in transplanted scaffold-free chondrocyte sheets using a minipig model. Biomaterials 2012;33:3846–51.
[37] Yamato M, Utsumi M, Kushida Konno AC, Kikuchi A, Okano T. Thermoresponsive culture dishes allow the intact harvest of multilayered keratinocyte sheets without dispase by reducing temperature. Tissue Eng 2001;7: 473–80.
[38] Mihara M, Higo S, Uchiyama Y, Tanabe K, Saito K. Different effects of high molecular weight sodium hyaluronate and NSAID on the progression of the cartilage degeneration in rabbit OA model. Osteoarthr Cartil 2007;15:543–9.
[39] Hayami T, Funaki H, Yaoeda K, Mitui K, Yamagiwa H, Tokunaga K, et al. Expression of the cartilage-derived anti-angiogenic factor chondromodulin-I decreases in the early stage of experimental osteoarthritis. J Rheumatol 2003;30:2207–17.
[40] O'Driscoll SW, Keeley FW, Salter RB. Durability of regenerated articular cartilage produced by free autogenous periosteal grafts in major full-thickness defects in joint surfaces under the influence of continuous passive motion. A followup report at one year. J Bone Joint Surg Am 1998;70:595–606.
[41] Mainil-Varlet P, Aigner T, Brittberg M, Bullough P, Hollander A, Hunziker E, et al. Histological assessment of cartilage repair: a report by the Histology Endpoint Committee of the International Cartilage Repair Society (ICRS). J Bone Joint Surg Am 2003;85-A(Suppl 2):45–57.
[42] Ochi M, Uchio Y, Kawasaki K, Iwasa J. Transplantation of cartilage-like tissue made by tissue engineering in the treatment of cartilage defects of the knee. J Bone Joint Surg Br 2002;84:571–8.
[43] Hunziker EB, Rosenberg LC. Repair of partial-thickness defects in articular cartilage: cell recruitment from the synovial membrane. J Bone Joint Surg Am 1996;78:721–33.
[44] Koga H, Muneta T, Nagase T, Nimura A, Ju Y-J, Mochizuki T, et al. Comparison of mesenchymal tissues-derived stem cells for in vivo chondrogenesis: suitable conditions for cell therapy of cartilage defects in rabbit. Cell Tissue Res 2008;333:207–15.

Sato et al. BMC Musculoskeletal Disorders 2012, 13:51
http://www.biomedcentral.com/1471-2474/13/51

BMC
Musculoskeletal Disorders

RESEARCH ARTICLE Open Access

Human telomerase reverse transcriptase and glucose-regulated protein 78 increase the life span of articular chondrocytes and their repair potential

Masato Sato[1*], Kazuo Shin-ya[2], Jeong Ik Lee[3], Miya Ishihara[4], Toshihiro Nagai[1], Nagatoshi Kaneshiro[1], Genya Mitani[1], Hidetoshi Tahara[5] and Joji Mochida[1]

Abstract

Background: Like all mammalian cells, normal adult chondrocytes have a limited replicative life span, which decreases with age. To facilitate the therapeutic use of chondrocytes from older donors, a method is needed to prolong their life span.

Methods: We transfected chondrocytes with hTERT or GRP78 and cultured them in a 3-dimensional atelocollagen honeycomb-shaped scaffold with a membrane seal. Then, we measured the amount of nuclear DNA and glycosaminoglycans (GAGs) and the expression level of type II collagen as markers of cell proliferation and extracellular matrix formation, respectively, in these cultures. In addition, we allografted this tissue-engineered cartilage into osteochondral defects in old rabbits to assess their repair activity in vivo.

Results: Our results showed different degrees of differentiation in terms of GAG content between chondrocytes from old and young rabbits. Chondrocytes that were cotransfected with hTERT and GRP78 showed higher cellular proliferation and expression of type II collagen than those of nontransfected chondrocytes, regardless of the age of the cartilage donor. In addition, the in vitro growth rates of hTERT- or GRP78-transfected chondrocytes were higher than those of nontransfected chondrocytes, regardless of donor age. In vivo, the tissue-engineered cartilage implants exhibited strong repairing activity, maintained a chondrocyte-specific phenotype, and produced extracellular matrix components.

Conclusions: Focal gene delivery to aged articular chondrocytes exhibited strong repairing activity and may be therapeutically useful for articular cartilage regeneration.

Background

Osteoarthritis (OA), which is one of the most common, debilitating, and costly chronic disorders [1], is characterized by progressive degeneration or destruction of articular cartilage. Since the incidence of OA increases with age, the underlying mechanism of this disease may involve a loss of the capacity of chondrocytes to regenerate with age. In proliferative cells, telomeres from chromosomes gradually became shorter as a result of the DNA replication end problem. To prevent cessation of mitosis and premature cell death, telomerase is a ribonucleoprotein that is an enzyme which adds DNA sequence repeats (TTAGGG) to the 3' end of DNA strands in the telomere regions, which are found at the ends of chromosomes [2]. The telomerase allows for replacement of short bits of DNA known as telomeres, which are otherwise shortened when a cell divides via mitosis. In normal circumstances, without the presence of telomerase, if a cell divides recursively, at some point all the progeny will reach their Hayflick limit. With the presence of telomerase, each dividing cell can replace the lost bit of DNA, and any single cell can then divide unbounded. While this unbounded growth property has excited many researchers, caution is warranted in exploiting this property, as exactly this same unbounded growth is a crucial step in enabling cancerous growth. In immortal human tumor cells, the gene for the catalytic subunit of

* Correspondence: sato-m@is.icc.u-tokai.ac.jp
[1]Department of Orthopaedic Surgery, Surgical Science, Tokai University School of Medicine, 143 Shimokasuya, Isehara, Kanagawa 259-1193, Japan
Full list of author information is available at the end of the article

human telomerase reverse transcriptase (*hTERT*) is almost always derepressed [3]. Moreover, *hTERT* is not only an oncoprotein [2] but also a regulator of cellular differentiation [4,5].

As a result, immortalized human cells, such as epithelial and fibroblast cells [6] and chondrocytes [7,8], have been used as models of cellular aging. For example, Goldring [7] showed that primary human chondrocytes can be immortalized with retroviral transfection of 4 genes, including simian vacuolating virus 40 large T antigen and telomerase; however, stable transfection of *hTERT* in chondrocytes that are cultured in a monolayer allows maintenance of the proliferative capacity but not the chondrocyte phenotype. In contrast, Piera-Velazquez et al. [8] showed that exogenous expression of *hTERT* in chondrocytes that are cultured on polyhydroxyethylmethacrylate coated dishes increases their life span and maintains their chondrocyte phenotype. Thus, *hTERT* may extend the life span of chondrocytes.

Glucose-regulated protein 78 (GRP78) is a molecular chaperone in the endoplasmic reticulum (ER) that is induced by ER stress and prevents cell death as a result of homeostatic imbalance in the ER [9]. Although overexpression of *GRP78* can limit the damage from ER stress in normal tissues and organs, the natural induction of GRP78 in neoplastic cells also may promote cancer progression and drug resistance [10]. Since *GRP78* also is involved in the pathology of neurological diseases, such as Alzheimer's disease [11] and Parkinson's disease [12], GRP78 may have therapeutic cytoprotective effects to limit ER stress.

To determine whether *hTERT* and *GRP78* can prolong the life span of chondrocytes and stimulate cartilage regeneration, we transfected rabbit articular chondrocytes with these genes and redifferentiated chondrocytes in a 3-dimensional atelocollagen honeycomb-shaped scaffold with a membrane seal (ACHMS scaffold) [13]. We used this type of scaffold because it is biodegradable, supports the growth of high-density cell cultures, and maintains the phenotype of articular chondrocytes [14-16]. In addition, to investigate the clinical relevance of our model to OA, we investigated whether the effects of gene transfection depend on the age of the cartilage by analyzing the proliferation, gross morphology, cellular content of DNA and proteoglycans, and gene expression level of type II collagen in the transfected chondrocytes.

Methods

Preparation of chondrocytes

All animal experiments in this study approved by Research Support and Intellectual Property of the University of Tokyo were performed in accordance with their institutional guidelines for the care and use of laboratory animals.

Chondrocytes were prepared as described previously [14]. Briefly, articular cartilage tissue specimens were collected from the knee and shoulder joints of 4 young male (4 weeks old, 1 kg) and 8 old female (4 years old, 4.5 kg) Japanese white rabbits (Tokyo Laboratory Animals Science Co., Ltd., Tokyo, Japan). Each rabbit specimen was soaked and stored separately in basal medium (BM) containing Dulbecco's modified Eagle's medium (DMEM)/F12 (Gibco; Invitrogen, Carlsbad, CA, USA) supplemented with 10% heat-inactivated fetal bovine serum (FBS) (Gibco), 50 $\mu g \cdot mL^{-1}$ ascorbic acid (Wako Pure Chemical Industries, Osaka, Japan), and 1% Fungizone® antibiotic-antimycotic solution (10,000 $U \cdot mL^{-1}$ penicillin G, 10 $mg \cdot mL^{-1}$ streptomycin sulfate, and 25 $\mu g \cdot mL^{-1}$ amphotericin B; Gibco). When needed, cartilage samples were chopped into small pieces, and then digested for 1 h in DMEM/F12 containing 0.4% pronase E (Kaken Pharmaceutical, Tokyo, Japan), followed by digestion for 3 h at 37°C in DMEM/F12 containing 0.016% collagenase P (Roche Diagnostics, Mannheim, Germany). Subsequently, the digested samples were filtered with a cell strainer (BD Falcon™; BD Bioscience, Bedford, MA, USA) with a 100 μm pore size and the isolated cells were rinsed twice with chilled Dulbecco's calcium- and magnesium-free, phosphate-buffered saline (PBS) (Dainippon Pharmaceutical, Osaka, Japan). The number of viable chondrocytes was counted by using a Burker-Turk hemocytometer (Erma, Tokyo, Japan) with Trypan blue staining. Finally, the chondrocytes were seeded in 500 cm^2 square dishes (245 mm × 245 mm; Corning, Corning, NY, USA) at a density of 10,000 $cells \cdot cm^{-2}$ and cultured in BM with 10% FBS at 37°C in an incubator with 5% CO_2.

Retroviral transfection

Retroviral transfection of cultured chondrocytes was performed as described previously [17,18] with some modifications. First, DH5α *Escherichia coli* cells (from Hiroshima University Graduate School of Biomedical Sciences) were cultured overnight in lysogeny broth (LB) media [19] at 37°C. Subsequently, these cells were transfected with p*hTERT*-MSCV and p*GRP78*-MSCV plasmids to produce amphotropic viruses. The plasmids were amplified and purified by using an EndoFree Plasmid Maxi Kit (Qiagen, Tokyo, Japan). In addition, the sequence of all constructs was verified by DNA sequencing.

Next, these plasmids were used to produce retroviral constructs by using 2 different protocols. To produce the *hTERT* retroviral construct, full-length *hTERT* cDNA was polymerase chain reaction (PCR) amplified, and then cloned into the pMSCV-puro retroviral vector (Clontech, Mountain View, CA, USA). Subsequently, the cloned vector was transfected into the Retropack PT67 (Clontech) packaging cell line and the transfected cells were selected with puromycin (1.8 $\mu g \cdot mL^{-1}$) (Sigma

Aldrich, St. Louis, MO, USA) after 48 h. Two weeks after transfection, the surviving cells were trypsinized and allowed to continue to grow for up to 100 d. The culture supernatant from this cell line was collected and 0.45-μm filtered, and then polybrene (8 $\mu g \cdot mL^{-1}$) was added prior to transducing *hTERT* into young rabbit (YRA) and old rabbit (ORA) chondrocyte cultures.

Chondrocytes were cultured and plated 24 h before viral infection. Then, the packaged retrovirus was added to the culture media and incubated at 37°C in an incubator with 5% CO_2. The infected cells were selected with 0.5 $\mu g \cdot mL^{-1}$ of puromycin (Sigma Chemical) for 7-10 d prior to subsequent experiments.

To produce the *GRP78* retroviral construct, full-length *GRP78* cDNA was PCR amplified, and then inserted into the mouse stem cell virus (MSCV) packaging vector by using the Retrovirus Packaging Kit Ampho (TaKaRa Biotechnology, Shiga City, Japan) [20]. To produce *GRP78*-expressing retroviruses, 293 T cells (CRL-11268™, ATCC, Manassas, VA, USA) were seeded and maintained on 6-cm dishes at a density of 400,000 $cells \cdot cm^{-2}$ in DMEM containing 10% FBS for 24 h prior to transfection. Then, the culture medium was changed to the same medium. Subsequently, the 293 T cells were co-transfected with pGP (gag-pol) and pE-ampho (env) (TaKaRa Biotechnology) by using calcium phosphate transfection. Transfected cells were selected with 400 $\mu g \cdot mL^{-1}$ of hygromycin (Calbiochem, La Jolla, CA, USA) and 50 μg of mycophenolic acid (Sigma Aldrich). After 48 h, the culture medium, which contained the recombinant retroviruses, was 0.45-μm filtered, and then mixed with DMEM to infect YRA and ORA chondrocyte cultures.

Chondrocyte proliferation

Chondrocyte proliferation was measured by counting cell numbers at 100% confluence in serial passages. Briefly, nontransfected or *hTERT*/*GRP78*-transfected YRA and ORA chondrocytes, which were passaged once every 7-10 d, were detached by using 0.05% trypsin/ethylenediaminetetraacetic acid (EDTA; Gibco) for 20-30 min at 37°C and washed 3 times with PBS. An aliquot of the detached cells was used to count the mean number of cells from 6 dishes by using a Burker-Turk hemocytometer (Erma) with Trypan blue staining. The remaining cells were replated at a density of 5×10^3 $cells \cdot well^{-1}$.

Cell proliferation was expressed as the population doubling level (PDL). The PDL was calculated from log-phase growth curves by using the equation: $PDL = \log_{10}(N/N_0) \times 3.33$, where N_0 and N are the number of cells at the beginning and end of each experiment, respectively [21].

Preparation of the atelocollagen honeycomb-shaped scaffold with a membrane seal and 3-dimensional culture of chondrocytes

The ACHMS scaffold was prepared as described previously [13] by Koken (Tokyo, Japan). Briefly, nontransfected and *hTERT*/*GRP78*-transfected ORA chondrocytes were passaged twice, and then seeded at a density of 2×10^6 $cells \cdot scaffold^{-1}$ into a round ACHMS scaffold (diameter, 6 mm; thickness, 2 mm; average pore size, 200 μm) [13,14,22,23] in 48-well plates (Sumitomo Bakelite, Tokyo, Japan) by centrifuging at 45 *g* for 5 min. Then, these cell-seeded scaffolds were cultured in BM supplemented with 10% FBS at 37°C in an incubator with 5% CO_2 and 100% relative humidity for 14 d. These cultured chondrocytes were frozen in liquid nitrogen until needed for biochemical analyses and transplantation into an in vivo model of articular cartilage defects.

Measurement of DNA and glycosaminoglycans

The amount of DNA in the cultured ORA chondrocytes, which was used as a marker of cell proliferation, was measured by digesting cell-seeded scaffolds with papain, and then using a fluorimetric assay, as described previously [24]. Briefly, 15 μL of a papain digest was mixed with 300 μL of Hoechst 33258 solution (Polyscience, Warrington, PA, USA), and then a Titertek Multiscan Spectrofluorometer (Lab Systems, Helsinki, Finland) was used to measure the emission and excitation spectra at 456 nm and 365 nm, respectively. DNA concentrations were calculated from a standard curve of calf thymus DNA (Sigma).

The amount of glycosaminoglycans (GAGs) in the cultured chondrocytes, which was used as a marker of extracellular matrix (ECM) formation, was quantified by using 1,9-dimethylmethylene blue, as described previously [25]. Briefly, samples (140 μL) of each chondrocyte culture were mixed gently with an equal volume of 1,9-dimethylmethylene blue solution in a 96-well microtiter plate, and then the absorbance at 530 nm was measured with a Titertec multiscan spectrophotometer (Labsystem, Helsinki, Finland). The amount of GAGs was calculated from the absorbance values by using a standard curve of 0.625-20 $\mu g \cdot mL^{-1}$ shark chondroitin sulfate C (Seikagaku Kogyo Co, Tokyo, Japan).

Type II collagen mRNA expression

Frozen 3-dimensional cultures of ORA chondrocytes were pulverized with a Cryo-Press (Microtec Nition, Chiba, Japan) in liquid nitrogen. All oligonucleotide primer sets were designed on the basis of published mRNA sequences. The expected amplicon lengths ranged from 70 to 200 bp. Cloning of the entire coding region of type 2 collagen was performed by 5'- and 3'-rapid amplification of cDNA ends

using the following oligonucleotide primers: forward (5'-AACACTGCCAACGTCCAGAT-3'), reverse (5'-CTGC AGCACGGTATAGGTGA-3'). Real-time PCR was performed in a SmartCycler system (Cepheid, Sunnyvale, CA) with SYBR Green PCR Master Mix (Applied Biosystems, Foster City, CA) with 1 μL of cDNA template in a final volume of 25 μL. Amplification of cDNA was performed according to the following conditions: 95°C for 15 s and 60°C for 60 s for 35-45 amplification cycles. Changes in the fluorescence of SYBR Green were monitored after every cycle. Melting curve analysis was performed through a 0.5°C/s increase from 55 to 95°C with continuous fluorescence readings at the end of the cycles to ensure that single PCR products were obtained. All reactions were repeated in six separate PCR runs using RNA isolated from four sets of human samples. The results were evaluated by using SmartCycler software (Cepheid). Glyceraldehyde-3-phosphate dehydrogenase (GAPDH) primers were used to normalize the samples. To monitor crossover contaminations of PCR, RNase-free water (Qiagen, Valencia, CA) was used in the RNA extraction and as a negative control. To ensure the quality of data, a negative control was always included in each run.

Implantation of tissue-engineered cartilage produced from transfected aged chondrocytes

Twenty four old female Japanese white rabbits were divided into 4 groups (control 8w, 16w; hTERT + GRP78 8w, 16w) and anesthetized with intramuscular injections of 120 mg of ketamine (Daiichisankyo, Tokyo, Japan) and 9 mg of xylazine (Bayer HealthCare, Leverkusen, Germany). After creating a medial parapatellar incision in both legs, each patella was dislocated laterally and a cylindrical defect (diameter, 5 mm; depth, 3 mm) was created on the patellar groove of the femur in both legs by using a biopsy punch (Kai Industries, Seki, Japan) and a low-speed drill (Takagi, Niigata, Japan). The bottom of the subchondral bone also was shaved to a plane until marrow bleeding was observed. Then, ACHMS scaffolds that were seeded with either nontransfected or *hTERT*/*GRP78*-transfected ORA chondrocytes were allografted into these defects without any fixatives, such as fibrin glue. Postoperatively, all animals were allowed to walk freely in their cages without any splints.

Postoperative analyses

Eight and 16 weeks after implantation, rabbits were killed with an overdose of intravenous anesthesia, and then the distal parts of their femurs were harvested and observed with a light microscope. Subsequently, the femur samples were fixed in 10% buffered formalin for 7 d. Each specimen was decalcified with 10% EDTA in distilled water (pH 7.4) for 3 weeks, and then embedded in paraffin, cut into 6-μm-thick sagittal sections, deparaffinized, and stained with safranin O (Cartilage Staining Kit, Takara, Shiga, Japan). The histopathology of the OA cartilage samples (n = 24) were analyzed according to standard grading and staging of OA cartilage histopathology [26]. The OA score was calculated by the following formula: OA score = most degenerated site in the cartilage (grades 1-6, Table 1) × area of degeneration (stages 1-4) (Table 2).

Immunohistochemical staining for type II collagen was performed as described previously [14]. Briefly, after deparaffinization, the sections were pretreated with 0.1 mg·mL^{-1} of actinase E (Kaken Pharmaceutical) in PBS at 37°C for 30 min. Then, the sections were incubated with 10% pig serum at room temperature for 30 min to reduce nonspecific background staining. These pretreated sections were incubated overnight with 50 mg·mL^{-1} mouse anti-human type II collagen monoclonal antibody (Daiichi Fine Chemical, Toyama, Japan) in PBS containing 0.1% bovine serum albumin at 4°C. Next, the sections were incubated with biotinylated rabbit anti-mouse immunoglobulin (1:500 dilution; Dako, Carpinteria, CA, USA) for 30 min at room temperature, followed by peroxidase-conjugated streptavidin (1:500 dilution; Dako) for 30 min at room temperature. Finally, the sections were incubated with a solution of 20 mg of diaminobenzidine and 5 μL of hydrogen peroxide (30%) in 100 mL of PBS for 5 min at room temperature. Control sections were incubated with PBS without any antibodies and stained in a similar manner. These sections were analyzed by light microscopy.

Statistical analysis

One-way analysis of variance and Dunn's post hoc test was used to determine statistical significance ($P < 0.05$).

Results

Establishment of primary cultures of rabbit chondrocytes

During the first 3 weeks, YRA, ORA, ORA + *hTERT*, and ORA + *hTERT* + *GRP78* chondrocytes showed similar growth rates for 10 PDL (Figure 1). Later, ORA + *hTERT* and ORA + *hTERT* + *GRP78* chondrocytes proliferated more rapidly than the nontransfected chondrocytes. However, YRA + *hTERT* + *GRP78* chondrocytes had the fastest growth rate. In the control groups, YRA chondrocytes proliferated faster than ORA chondrocytes during the entire observation period, but their growth rate gradually decreased until they ceased at about 40 d and 60 d after the initiation of culture, respectively. Unlike control cells, which stopped proliferating after 10-20 PDL, ORA + *hTERT* and YRA + *hTERT* cells continued proliferating for about 35 and 50 PDL, respectively. These results showed that *hTERT* and *GRP78* increase the growth rate of transfected cells approximately 3-fold compared with nontransfected cells.

Table 1 OA cartilage histopathology grade assessment; grading methodology

Grade (key feature)	Associated criteria (tissue reaction)
Grade 1: surface intact	Matrix: superficial zone intact, oedema and/or superficial fibrillation (abrasion), focal superficial matrix condensation Cells: death, proliferation (clusters), hypertrophy, superficial zone Reaction must be more than superficial fibrillation only
Grade 2: surface discontinuity	As above + Matrix discontinuity at superficial zone (deep fibrillation) ± Cationic stain matrix depletion (Safranin O or Toluidine Blue) upper 1/3 of cartilage ± Focal perichondronal increased stain (mid zone) ± Disorientation of chondron columns Cells: death, proliferation (clusters), hypertrophy
Grade 3: vertical fissures (clefts)	As above Matrix vertical fissures into mid zone, branched fissures ± Cationic stain depletion (Safranin O or Toluidine Blue) into lower 2/3 of cartilage (deep zone) ± New collagen formation (polarized light microscopy, Picro Sirius Red stain) Cells: death, regeneration (clusters), hypertrophy, cartilage domains adjacent to fissures
Grade 4: erosion	Cartilage matrix loss: delamination of superficial layer, mid layer cyst formation Excavation: matrix loss superficial layer and mid zone
Grade 5: denudation	Surface: sclerotic bone or reparative tissue including fibrocartilage within denuded surface. Microfracture with repair limited to bone surface
Grade 6: deformation	Bone remodelling (more than osteophyte formation only). Includes: microfracturewith fibrocartilaginous and osseous repair extending above the previous surface

Grade = depth progression into cartilage

Characteristics of the 3-dimensional cultures of chondrocytes

The ACHMS scaffold supported a high density of ORA chondrocytes (2×10^6 cells·cm^{-2}) without any leakage of cells. During the 2-week culture, the chondrocytes in the scaffold retained their normal spherical shape (data not shown) and the resulting tissue-engineered cartilage maintained its shape and size in the ACHMS scaffold. The scaffolds were elastic and did not deform during culturing or collapse when handled with forceps.

Figure 2 shows macroscopic images of the cell-seeded scaffolds after culturing for 14 d. The scaffold that was seeded with *hTERT/GRP78*-transfected ORA chondrocytes had the highest cell density. In addition, the spaces between the atelocollagen matrix were filled and not visible along the edge of the ACHMS scaffold, which indicated that chondrocytes had proliferated throughout the scaffold during the cultivation period. In the scaffolds that were seeded with control cells, cell growth was sparse, and as a result, the spaces between the atelocollagen matrix remained mostly empty.

Glycosaminoglycan content of cell-seeded scaffolds

On day 14, the amount of GAG in cell-seeded scaffolds differed significantly between each group (Figure 3). Specifically, the total GAG content of scaffolds that were seeded with *hTERT/GRP78*-transfected ORA chondrocytes was higher than those that were seeded with *GRP78*- or *hTERT*-transfected cells. In addition, the GAG content of the scaffolds that were seeded with transfected ORA chondrocytes was higher than that in those that were seeded with nontransfected chondrocytes. These results suggested that transfected ORA chondrocytes were able to produce and accumulate significantly higher amounts of extracellular matrix components in the ACHMS scaffold than nontransfected chondrocytes.

Table 2 OA score; semi-quantitative method

Grade (key feature)	Stage % Involvement (surface, area, volume)			
	Stage 1 < 10%	Stage 2 10-25%	Stage 3 25-50%	Stage 4 > 50%
Grade 1(surface intact)	1	2	3	4
Grade 2 (surface discontinuity)	2	4	6	8
Grade 3 (vertical fissures, clefts)	3	6	9	12
Grade 4 (erosion)	4	8	12	16
Grade 5(denudation)	5	10	15	20
Grade 6(deformation)	6	12	18	24

Score = grade × stage

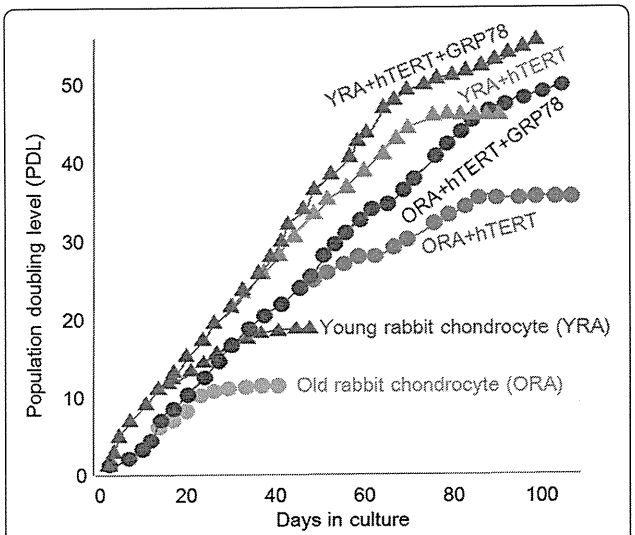

Figure 1 Effect of *hTERT* and *GRP78* on the proliferation of rabbit chondrocytes. Growth curves of cultures of nontransfected control chondrocytes from young and old rabbits (YRA and ORA, respectively) and *hTERT* (YRA + *hTERT* and ORA + *hTERT*) and *GRP78* (YRA + *hTERT* + *GRP78* and ORA + *hTERT* + *GRP78*)-transfected chondrocytes. The mean number of cells is shown on a $\log_{10}$ scale.

Type II collagen mRNA expression

As shown in Figure 4, the mRNA expression of type II collagen was observed in ORA, regardless of different gene transfection. Profiles of control, $GRP78^+$, $hTERT^+$, and $hTERT^+/GRP78^+$ cells were prepared to investigate expression of type II collagen. The mRNA expressions of $GRP78^+$, $hTERT^+$, and $hTERT^+/GRP78^+$ cells were significantly higher than that in control of non-transfective ORA. Chondrocytes are known to readily dedifferenciate in 2-dimensional culture. However, in this study, we used the primary culture of chondrocytes so that these chondrocytes retain their phenotype, which can be confirmed from type II collagen expression.

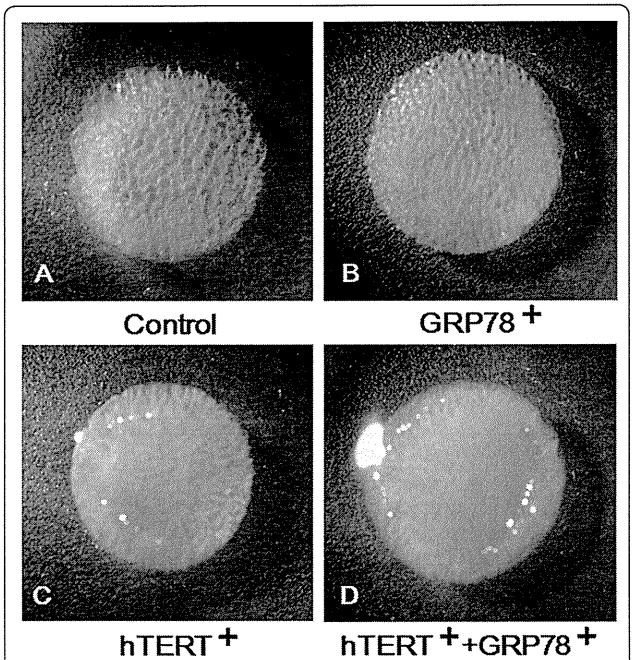

Figure 2 Macroscopic images of the cell-scaffold complex after 14 days of culture. Atelocollagen honeycomb-shaped scaffold with a membrane seal (ACHMS) scaffold complex seeded with nontransfected (A), *GRP78*-transfected (B), *hTERT*-transfected (C), or *hTERT*- and *GRP78*-transfected (D) ORA chondrocytes. Scale bar = 1.0 mm.

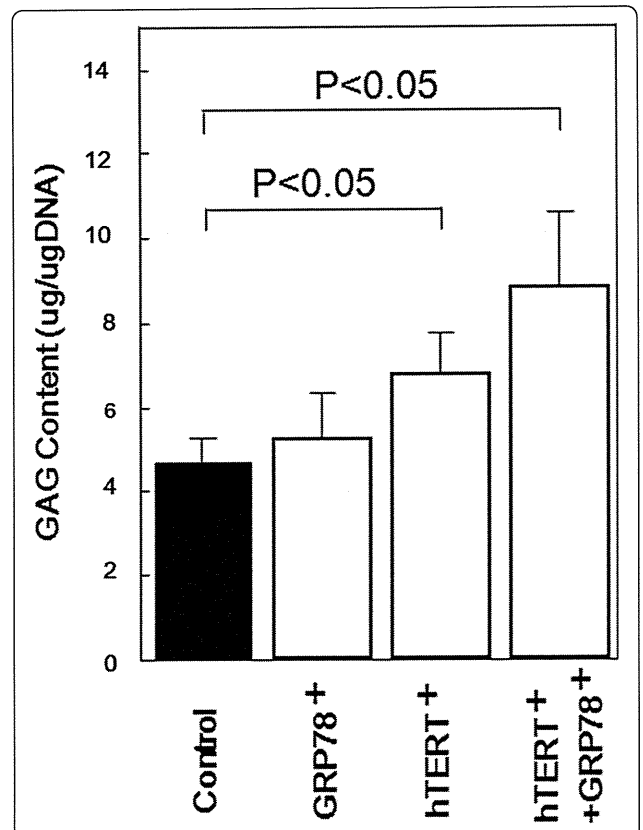

Figure 3 Glycosaminoglycan content of chondrocyte cultures in atelocollagen honeycomb-shaped scaffolds with a membrane seal. The glycosaminoglycan (GAG) content of nontransfected (black bars) or *hTERT*- or *GRP78*-transfected (white bars) ORA chondrocytes on the indicated days. Results are expressed as the mean (SD) of 6 independent measurements. *$P < 0.05$.

Macroscopic appearance of repaired osteochondral defects

The surgical implantation of tissue-engineered cartilage into osteochondral defects in the old rabbits was uneventful, and upon waking, all rabbits immediately resumed normal cage activity. At the time that they were killed, all rabbits exhibited unlimited passive range of motion in the knee joint.

Indeed, the osteochondral defects in old rabbits that were treated with tissue-engineered cartilage that was

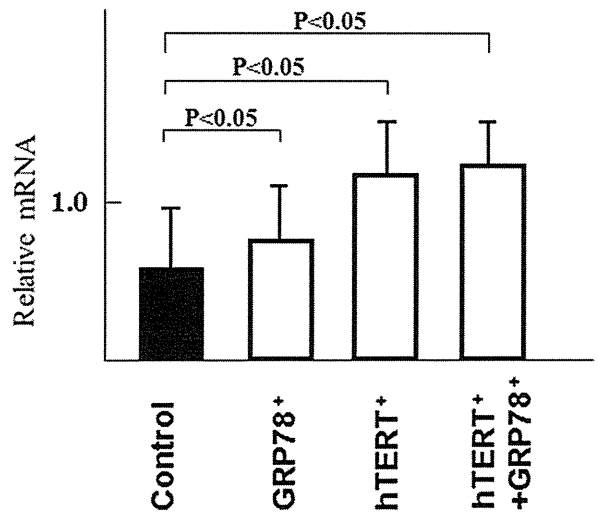

Figure 4 mRNA expression levels of type II collagen in transfected chondrocytes. The mRNA expression of type II collagen was observed in ORA, regardless of different gene transfection. Profiles of control, *GRP78*$^+$, *hTERT*$^+$, and *hTERT*$^+$/*GRP78*$^+$ cells were prepared to investigate expression of type II collagen. The mRNA expressions of *GRP78*$^+$, *hTERT*$^+$, and *hTERT*$^+$/*GRP78*$^+$ cells were significantly higher than that in control of non-transfective ORA. GAPDH was used as an internal control to normalize RNA levels.

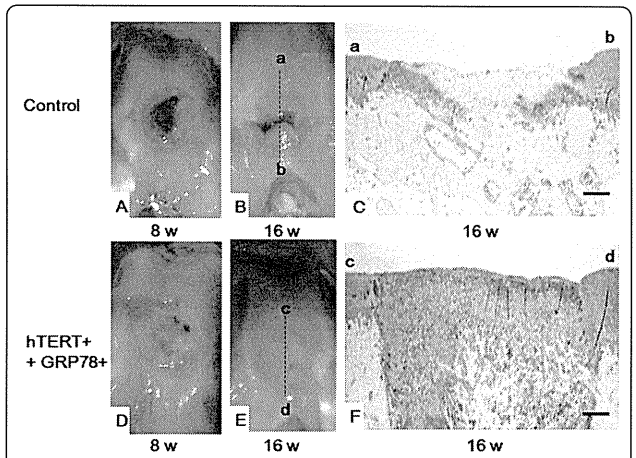

Figure 5 Macroscopic and immunostaining of regenerated cartilage after implantation. Postoperative appearance of repaired osteochondral defects in old rabbits implanted with scaffolds seeded with either nontransfected (top panels) or *hTERT*- and *GRP78*-transfected ORA chondrocytes (bottom panels) either 8 (A, D) or 16 (B, E) weeks after surgery. Immunostaining of type II collagen in tissue sections from rabbits implanted with scaffolds seeded with nontransfected (C) or *hTERT*- and *GRP78*-transfected (F) ORA chondrocytes. Each micrograph is representative of 8 tissue samples. Scale bar = 1.0 mm.

grown from *hTERT*- and *GRP78*-transfected ORA chondrocytes were filled with smooth tissue that resembled hyaline cartilage 16 weeks after surgery (Figure 5E) unlike the tissue-engineered cartilage that was grown from nontransfected ORA chondrocytes, which remained empty or were covered by fibrous tissue (Figure 5B). Although the control tissue-engineered cartilage showed some tissue repair along the borders of the defect, the color of the tissue was slightly different from that of the surrounding normal cartilage (Figure 5A, B).

Histological analysis of repaired osteochondral defects

No signs of arthritis, such as cartilage erosion or severe synovial proliferation, were observed in any surgically treated knee. In rabbits that were implanted with tissue-engineered cartilage grown from *hTERT*- and *GRP78*-transfected ORA chondrocytes, the immunohistochemical staining for type II collagen in the extracellular matrix in the scaffold was more intense and covered a larger area (Figure 5F) than those that were implanted with scaffolds that were grown from nontransfected ORA chondrocytes (Figure 5C). In addition, the tissue-engineered cartilage that was grown from transfected ORA chondrocytes was smooth and displayed good bonding with the host cartilage on both sides. In contrast, the tissue-engineered cartilage that was grown from nontransfected ORA chondrocytes had an irregular surface and was thinner than that grown from *hTERT*- and *GRP78*-transfected chondrocytes (Figure 5C).

As shown in Figure 6, the average OA scores were as follows: control 8w, 11.2 (2.5); 16w, 16.0 (3.2); hTERT + GRP78 8w, 17.3 (3.5); 16w, 21.00 (2.85). Statistically significant differences ($P < 0.05$) were observed between the transfected and nontransfected groups that were observed for the same period of time after implantation.

Discussion

Aging is the most important risk factor for both the initiation and progression of degenerative cartilage diseases. Osteoarthritic cartilage degeneration may be due to the loss of viable chondrocytes due to apoptosis or physical stress. This degeneration is likely to be closely related to age-related changes, since aging chondrocytes and articular cartilage matrix undergo senescence-like changes, which increase the susceptibility of cells to degenerative processes and environmental or physiological stresses [27]. As a result, chondrocytes from osteoarthritic patients might progress toward senescence more rapidly than those from normal individuals.

Aging chondrocytes also have important therapeutic ramifications. Recently, the treatment of articular cartilage defects have improved with the introduction of advanced tissue engineering techniques for autologous chondrocyte implantation (ACI) [28]. ACI requires cell expansion in culture to provide sufficient amounts of chondrocytes for reimplantation. However, like all mammalian cells, normal adult chondrocytes have a limited mitotic potential and eventually enter a state of senescence [29]. Moreover, the

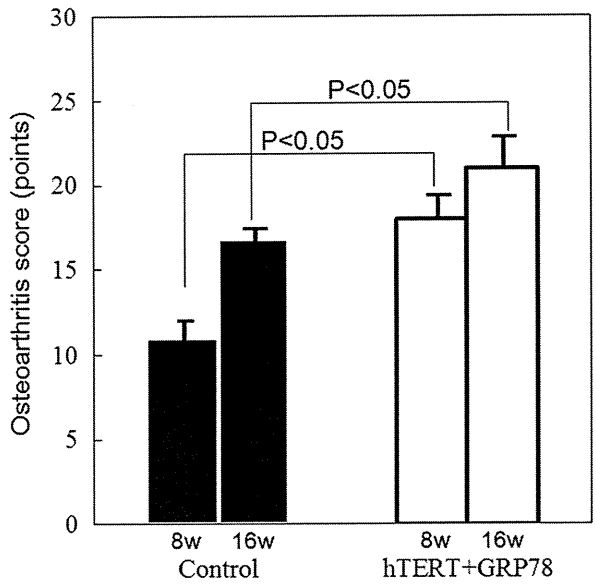

Figure 6 Osteoarthritis score. The histopathology of the OA cartilage samples from all 4 groups (n = 24) were analyzed according to standard grading and staging of OA cartilage histopathology. OA scores were calculated by using the following formula: OA score = most degenerated site in the cartilage (grades 1-6, Table 1) × area of degeneration (stages 1-4) (Table 2). Error bars indicate the standard deviation of each group. Statistically significant differences were observed between the control and hTERT + GRP78 groups 8 and 16 weeks after transplantation.

replicative life span of primary cells in culture are affected by the age of the donor, such that cells from older donors have a shorter life spans than those from younger donors [30]. For example, in monolayer cultures of aged human chondrocytes, serial passages rapidly results in loss of phenotypic stability and proliferative capacity [7]. Thus, to facilitate the therapeutic use of chondrocytes from older donors, a method is needed to prolong their replicative life span.

One possible method is transfection of *hTERT*, which can immortalize or prolong the life span of various human cells, such as muscle satellite cells [31,32], myoblasts [33,34], fibroblasts [6], and chondrocytes [7,8]. Since most immortalized cells maintain their phenotype and state of differentiation, *hTERT*-transfected cells are considered potential therapies for small-cell lung cancer [35] and for postnatal neovascularization in severe ischemic disease [36]. However, since chondrocytes uniquely maintain their phenotypes in 3-dimensional cultures [37], it is not known whether *hTERT*-immortalized chondrocytes maintain their state of differentiation.

Due to the aforementioned issues, in most cartilage tissue engineering studies, donor chondrocytes are usually from young animals. Our study is the first report that transfection of *hTERT* and *GRP78* can increase the replicative life span and therapeutic potential of tissue-engineered cartilage that is produced from ORA chondrocytes, which have a limited regenerative capacity. In addition, we used an ACHMS scaffold to maintain the phenotype of transfected chondrocytes, as indicated by the production of GAGs and type II collagen (Figures 3 and 4). These results are consistent with the findings of Piera-Velazquez et al. [8].

In this study, we overcame the limited lifespan of ORA chondrocytes by transfection with *hTERT* and increased their growth rate up to 3-fold by cotransfection with *GRP78* (Figure 1). Specifically, *hTERT/GRP78*-transfected ORA chondrocytes grew at a constant rate for more than 20 PDL, whereas nontransfected chondrocytes stopped dividing after much fewer PDL. However, we were not able to completely immortalize chondrocytes, even those from young rabbits (PDL < 50). Although the additional transfection of SV40-TAg or mutant Ras could immortalize these cells, we did not choose this option because the transfected cells may have become cancerous. As a result, we focused on the phenotypic stability of GRP78 and hTERT.

hTERT is a candidate gene for gene therapy of muscular dystrophy [31-34]. In contrast, *GRP78* may have therapeutic applications for neuropathological conditions, such as Alzheimer's disease, because it protects cells from ER stress [11,38-40]. ER stress can alter protein synthesis in cells [41]. One mechanism by which ER stress promotes apoptosis in cells is by driving the accumulation of structurally abnormal proteins [42], which are ordinarily repaired by ER chaperones to prevent age-related cell death. GRP78 is an example of a chaperone protein that regulates protein folding in the ER and thus contributes to cell survival [43]. Since the increase in the expression of GRP78 during cell culture may help protect cells from ER stress, overexpression of GRP78 also may protect cultured chondrocytes independent of hTERT.

Due to a lack of cages for mutant rabbits, we were not able to perform animal transplantation experiments with chondrocytes that were transfected with *hTERT* or *GRP78* alone. However, we believe that our in vitro and in vivo results from chondrocytes that were transfected with both *hTERT* and *GRP78* are sufficient to support our conclusions. In the future, we plan to perform more animal experiments to elucidate the effects of *GRP78*.

In conclusion, our results showed that tissue-engineered cartilage that was grown from implanted *in vivo* with *hTERT*- and *GRP78*-transfected ORA chondrocytes in ACHMS scaffolds can repair articular cartilage defects in vivo (Figure 5D, E, F). The *hTERT* and *GRP78*-transfected ORA exhibited proliferative and differentiation activity in articular cartilage defects, resulting in the formation of hyaline cartilage. This study also shows that ORA chondrocytes potentially produce hyaline cartilage after genetic treatment, similar to chondrocytes from young animals.

However, the mechanical strength of regenerated articular cartilage in large animals (*i.e.*, sheep or pigs) needs to be investigated.

Abbreviations

hTERT: Human telomerase reverse transcriptase; GRP78: Glucose-regulated protein 78; ER: Endoplasmic reticulum; ACHMS scaffold: Atelocollagen honeycomb-shaped scaffold with a membrane seal; OA: Osteoarthritis; BM: Basal medium; DMEM: Dulbecco's modified Eagle's medium; FBS: Fetal bovine serum; YRA: Young rabbit; ORA: Old rabbit; PDL: Population doubling level; RT-PCR: Reverse transcriptase-polymerase chain reaction; GAPDH: Gylceraldehyde-3-phosphate dehydrogenase; ACI: Autologous chondrocyte implantation; ECM: Extracellular matrix.

Acknowledgements

This work was supported by the Takeda Science Foundation, Grant of the New Energy and Industrial Technology Development Organization, and High-Tech Research Center Project 2004 for Private University. The funders had no role in study design, data collection and analysis, decision to publish, or preparation of the manuscript.

Author details

[1]Department of Orthopaedic Surgery, Surgical Science, Tokai University School of Medicine, 143 Shimokasuya, Isehara, Kanagawa 259-1193, Japan. [2]Biomedicinal Information Research Center, National Institute of Advanced Industrial Science and Technology (AIST), 2-42 Aomi, Koto-ku, Tokyo 135-0064, Japan. [3]Department of Biomedical Science & Technology, Institute of Biomedical Science & Technology (IBST), Konkuk University, 1 Hwang-dong, Gwangjin-gu, Seoul 143-701, Korea. [4]Department of Medical Engineering, National Defense Medical College, 3-2 Namiki, Tokorozawa, Saitama 359-8513, Japan. [5]Hiroshima University Graduate School of Biomedical Sciences, 1-2-3 Kasumi, Minami-ku, Hiroshima 734-8553, Japan.

Authors' contributions

MS, KS, MI, and TN conducted the experiments. MS, MI, NK, TK, HT, and GM analyzed the data. JIL performed the statistical analyses. MS, JIL, and JM wrote the manuscript. All authors read and approved the final manuscript.

Competing interests

The authors declare that they have no competing interests.

Received: 3 November 2011 Accepted: 2 April 2012
Published: 2 April 2012

References

1. Issa SN, Sharma L: **Epidemiology of osteoarthritis: an update.** *Curr Rheumatol Rep* 2006, **8**:7-15.
2. Harley CB: **Telomerase is not an oncogene.** *Oncogene* 2002, **21**:494-502.
3. Meyerson M, Counter CM, Eaton EN, Ellisen LW, Steiner P, Caddle SD, Ziaugra L, Beijersbergen RL, Davidoff MJ, Liu Q, Bacchetti S, Haber DA, Weinberg RA: **hEST2, the putative human telomerase catalytic subunit gene, is up-regulated in tumor cells and during immortalization.** *Cell* 1997, **90**:785-795.
4. Mattson MP, Fu W, Zhang P: **Emerging roles for telomerase in regulating cell differentiation and survival: a neuroscientist's perspective.** *Mech Ageing Dev* 2001, **122**:659-671.
5. Liu L, DiGirolamo CM, Navarro PA, Blasco MA, Keefe DL: **Telomerase deficiency impairs differentiation of mesenchymal stem cells.** *Exp Cell Res* 2004, **294**:1-8.
6. Hahn WC, Counter CM, Lundberg AS, Beijersbergen RL, Brooks MW, Weinberg RA: **Creation of human tumour cells with defined genetic elements.** *Nature* 1999, **400**:464-468.
7. Goldring MB: **Immortalization of human articular chondrocytes for generation of stable, differentiated cell lines.** *Methods Mol Med* 2004, **100**:23-36.
8. Piera-Velazquez S, Jimenez SA, Stokes D: **Increased life span of human osteoarthritic chondrocytes by exogenous expression of telomerase.** *Arthritis Rheum* 2002, **46**:683-693.
9. Reddy RK, Mao C, Baumeister P, Austin RC, Kaufman RJ, Lee AS: **Endoplasmic reticulum chaperone protein GRP78 protects cells from apoptosis induced by topoisomerase inhibitors: role of ATP binding site in suppression of caspase-7 activation.** *J Biol Chem* 2003, **278**:20915-20924.
10. Lee AS: **The glucose-regulated proteins: stress induction and clinical applications.** *Trends Biochem Sci* 2001, **26**:504-510.
11. Katayama T, Imaizumi K, Manabe T, Hitomi J, Kudo T, Tohyama M: **Induction of neuronal death by ER stress in Alzheimer's disease.** *J Chem Neuroanat* 2004, **28**:67-78.
12. Ryu EJ, Harding HP, Angelastro JM, Vitolo OV, Ron D, Greene LA: **Endoplasmic reticulum stress and the unfolded protein response in cellular models of Parkinson's disease.** *J Neurosci* 2002, **22**:10690-10698.
13. Sato M, Asazuma T, Ishihara M, Kikuchi T, Masuoka K, Ichimura S, Kikuchi M, Kurita A, Fujikawa K: **An atelocollagen honeycomb-shaped scaffold with a membrane seal (ACHMS-scaffold) for the culture of annulus fibrosus cells from an intervertebral disc.** *J Biomed Mater Res A* 2003, **64**:248-256.
14. Masuoka K, Asazuma T, Ishihara M, Sato M, Hattori H, Ishihara M, Yoshihara Y, Matsui T, Takase B, Kikuchi M, Nemoto K: **Tissue engineering of articular cartilage using an allograft of cultured chondrocytes in a membrane-sealed atelocollagen honeycomb-shaped scaffold (ACHMS scaffold).** *J Biomed Mater Res B Appl Biomater* 2005, **75**:177-184.
15. Ishihara M, Sato M, Sato S, Kikuchi T, Mochida J, Kikuchi M: **Usefulness of photoacoustic measurements for evaluation of biomechanical properties of tissue-engineered cartilage.** *Tissue Eng* 2005, **11**:1234-1243.
16. Glowacki J, Mizuno S: **Collagen scaffolds for tissue engineering.** *Biopolymers* 2008, **89**:338-344.
17. Pear WS, Nolan GP, Scott ML, Baltimore D: **Production of high-titer helper-free retroviruses by transient transfection.** *Proc Natl Acad Sci USA* 1993, **90**:8392-8396.
18. Fujita T, Otsuka-Tanaka Y, Tahara H, Ide T, Abiko Y, Mega J: **Establishment of immortalized clonal cells derived from periodontal ligament cells by induction of the hTERT gene.** *J Oral Sci* 2005, **47**:177-184.
19. Bertani G: **Lysogeny at mid-twentieth century: P1, P2, and other experimental systems.** *J Bacteriol* 2004, **186**:595-600.
20. Hawley RG, Lieu FH, Fong AZ, Hawley TS: **Versatile retroviral vectors for potential use in gene therapy.** *Gene Ther* 1994, **1**:136-138.
21. Cristofalo VJ, Allen RG, Pignolo RJ, Martin BG, Beck JC: **Relationship between donor age and the replicative lifespan of human cells in culture: a reevaluation.** *Proc Natl Acad Sci USA* 1998, **95**:10614-10619.
22. Itoh H, Aso Y, Furuse M, Noishiki Y, Miyata T: **A honeycomb collagen carrier for cell culture as a tissue engineering scaffold.** *Artif Organs* 2001, **25**:213-217.
23. Hattori H, Sato M, Masuoka K, Ishihara M, Kikuchi T, Matsui T, Takase B, Ishizuka T, Kikuchi M, Fujikawa K, Ishihara M: **Osteogenic potential of human adipose tissue-derived stromal cells as an alternative stem cell source.** *Cells Tissues Organs* 2004, **178**:2-12.
24. Kim YJ, Sah RL, Doong JY, Grodzinsky AJ: **Fluorometric assay of DNA in cartilage explants using Hoechst 33258.** *Anal Biochem* 1988, **174**:168-176.
25. Farndale RW, Buttle DJ, Barrett AJ: **Improved quantitation and discrimination of sulphated glycosaminoglycans by use of dimethylmethylene blue.** *Biochim Biophys Acta* 1986, **883**:173-177.
26. Pritzker KP, Gay S, Jimenez SA, Ostergaard K, Pelletier JP, Revell PA, Salter D, van den Berg WB: **Osteoarthritis cartilage histopathology: grading and staging.** *Osteoarthritis Cartilage* 2006, **14**:13-29.
27. Aigner T, Rose J, Martin J, Buckwalter J: **Aging theories of primary osteoarthritis: from epidemiology to molecular biology.** *Rejuvenation Res* 2004, **7**:134-145.
28. Brittberg M, Lindahl A, Nilsson A, Ohlsson C, Isaksson O, Peterson L: **Treatment of Deep Cartilage Defects in the Knee with Autologous Chondrocyte Transplantation.** *N Engl J Med* 1994, **331**:889-895.
29. Evans CH, Georgescu HI: **Observations on the senescence of cells derived from articular cartilage.** *Mech Ageing Dev* 1983, **22**:179-191.
30. Hayflick L: **The limited in vitro lifetime of human diploid cell strains.** *Exp Cell Res* 1965, **37**:614-636.
31. Cudre-Mauroux C, Occhiodoro T, Konig S, Salmon P, Bernheim L, Trono D: **Lentivector-mediated transfer of Bmi-1 and telomerase in muscle satellite cells yields a duchenne myoblast cell line with long-term genotypic and phenotypic stability.** *Hum Gene Ther* 2003, **14**:1525-1533.
32. Di Donna S, Renault V, Forestier C, Piron-Hamelin G, Thiesson D, Cooper RN, Ponsot E, Decary S, Amouri R, Hentati F, Butler-Browne GS, Mouly V: